

# Bayesian inference from rank data

Øystein Sørensen<sup>\*1</sup>, Valeria Vitelli<sup>†1</sup>, Arnaldo Frigessi<sup>‡1,2</sup>, and Elja Arjas<sup>§1,3</sup>

<sup>1</sup>Oslo Centre for Biostatistics and Epidemiology, Department of Biostatistics,  
University of Oslo, Norway

<sup>2</sup>Oslo Centre for Biostatistics and Epidemiology, Research Support Services, Oslo  
University Hospital, Norway

<sup>3</sup>Department of Mathematics and Statistics, University of Helsinki, Finland

December 6, 2024

## Abstract

Modeling and analysis of rank data have received renewed interest in the era of big data, when recruited and volunteer assessors compare and rank objects to facilitate decision making in disparate areas, from politics to entertainment, from education to marketing. The Mallows rank model is among the most successful approaches, but its use has been limited to a particular form based on the Kendall distance, for which the normalizing constant has a simple analytic expression. In this paper, we develop computationally tractable methods for performing Bayesian inference in Mallows models with any right-invariant metric, thereby allowing for greatly extended flexibility. Our methods also allow to estimate consensus rankings for data in the form of top- $t$  rankings, pairwise comparisons, and other linear orderings. In addition, clustering via mixtures allows to find substructure among assessors. Finally we construct a regression framework for ranks which vary over time. We illustrate and investigate our approach on simulated data, on performed experiments, and on benchmark data.

**Keywords**— Highly structured stochastic systems, incomplete rankings, Mallows model, pairwise comparisons, preference learning

## 1 Introduction

Various types of data have ranks as their natural scale. Students applying to secondary or university education rank prospective schools or colleges, and are usually admitted based on a ranking built on their past results. The manufacturing industry recruits panels to rank novel products, like food with new flavours. Market studies are often based on interviews where competing products are compared and ranked. In the era of big data, analysing preference data (e.g., movie preferences, restaurant rankings, ...) receives much attention. In addition to these examples, where rankings or preferences are the natural quantitative units, converting continuous

---

\*oystein.sorensen@medisin.uio.no

†valeria.vitelli@medisin.uio.no

‡arnaldo.frigessi@medisin.uio.no

§earjas@mappi.helsinki.fi

data to ranks can lead to more robust inference when absolute scales are not easily comparable, as in the case of genomic data. For example, Afsari et al. (2014) classify phenotypes based on ranked RNA expressions, and the ARACNE algorithm (Margolin et al., 2006) uses ranked mutual information between pairs of genes to reconstruct gene regulatory networks. For the general background on statistical methods for rank data up to the mid 1990’s, we refer to the excellent monograph by Marden (1995).

Two of the most used models are the classical Plackett-Luce (Luce, 1959; Plackett, 1975) and Mallows models (Mallows, 1957). There is a growing literature on preference learning based on these models. For example, Caron and Teh (2012) do Bayesian inference in a Plackett-Luce model with time-dependent preferences, and further develop the framework in Caron et al. (2014), where a Dirichlet process mixture is used to cluster assessors based on their preferences. In the Mallows model, Meilă and Chen (2010) use a Dirichlet process mixtures to perform clustering, and Lu and Boutilier (2011) cluster via the EM algorithm, while also allowing for data in the form of pairwise preferences.

Remarkably, most of the work on Mallows models has been limited to *one particular form* of the model which uses the Kendall distance. For this metric, the normalizing constant of the Mallows distribution can be computed analytically. Fligner and Verducci (1986) introduced the Generalized Mallows model, which models the ranking process more closely, and of which the Mallows model with the Kendall distance is a special case. A Bayesian treatment of this model is given in Fligner and Verducci (1990). However, many other metrics, like the footrule and the Spearman distance, can be used. Except for computational considerations, there is no reason to assume that these metrics are less powerful than Kendall’s.

In this paper, we develop a Bayesian framework for inference in Mallows models with any right-invariant metric. The normalizing constant is computed offline, using an efficient importance sampling scheme. Full Bayesian inference is based on a Metropolis-Hastings algorithm designed for rank data. Using data augmentation techniques, our methods also allow for incomplete data like top- $t$  rankings, pairwise comparisons, and ranks which are missing at random. We also perform clustering of assessors via mixtures, and model ranks which are varying over time. One advantage of our method is the option to use different metrics, while still performing clustering and allowing for various types of partial data. By being fully Bayesian, all uncertainty in the model is taken into account in the posterior distributions, and relevant prior knowledge can be represented in the prior distribution.

In Section 2, we introduce the Bayesian Mallows model for rank data, give an overview of previous work, and discuss modelling issues like the choice of distance measure and prior distribution. In Section 3, we show how efficient Bayesian computation can be performed for this model, by using a novel leap-and-shift distribution to propose ranks in the Metropolis-Hastings algorithm. We also develop an importance sampling scheme for computing the normalizing constant. Section 4 presents our *potato experiment*, which illustrates the use of the Mallows model for data in the form of full rankings.

In Section 5 we extend our model in order to partial rankings. Section 6 considers data in the form of ordered subsets or pairwise comparisons of items. In Section 7 we cluster the assessors via mixture distributions, and in Section 8 we analyze ranks which vary over time. Each extension of the model is followed by a case study illustrating its use. We demonstrate how to handle top- $t$  rankings in the potato experiment, compare football teams in a full season of the Premier League by using each game as a pairwise comparison, find clusters of consumers with similar taste preferences in a sushi dataset, and finally analyze how the ranking of a class of high school students based on math test scores varies over four years. In Section 9 we perform simulation experiments in order to gain further insight into how the model works when applying different distance measures.

## 2 A Bayesian Mallows model for ranks

Assume we have a set of  $n$  items, represented by  $\mathbf{A} = \{A_1, A_2, \dots, A_n\}$ , which each of  $N$  assessors is asked to rank individually with respect to a considered feature. The ordering provided by assessor  $j$  is represented by the vector  $\mathbf{X}_j$ , with  $n$  components, each being an item in  $\mathbf{A}$ . The item with rank 1 appears as the first element, up to the item with rank  $n$  appearing as the  $n$ th element. Our observations are now  $N$  permutations of the labels in  $\mathbf{A}$ , represented by  $\mathbf{X}_1, \dots, \mathbf{X}_N$ . Let

$$R_{ij} = \mathbf{X}_j^{-1}(A_i), \quad i = 1, \dots, n, \quad j = 1, \dots, N \quad (1)$$

denote the rank given to item  $A_i$  by assessor  $j$ , and let  $\mathbf{R}_j = (R_{1j}, R_{2j}, \dots, R_{nj})$ ,  $j = 1, \dots, N$  denote the full set of ranks given to the items by assessor  $j$ . Letting  $\mathcal{P}_n$  be the set of all permutations of  $\{1, \dots, n\}$ , we have  $\mathbf{R}_j \in \mathcal{P}_n$ ,  $j = 1, \dots, N$ . For a reference ordering  $\mathbf{Y}$  of the elements in  $\mathbf{A}$ , we let  $\rho_i = \mathbf{Y}^{-1}(A_i)$ ,  $i = 1, \dots, n$  be the rank of item  $A_i$ , and denote the corresponding vector of ranks by  $\boldsymbol{\rho} = (\rho_1, \rho_2, \dots, \rho_n) \in \mathcal{P}_n$ . Finally, let  $d(\cdot, \cdot) : \mathcal{P}_n \times \mathcal{P}_n \rightarrow [0, \infty)$  be a distance measure on the space of  $n$ -dimensional permutations.

Mallows models (Mallows, 1957) are a well-known class of non-uniform joint distributions for  $\mathbf{R}$  on  $\mathcal{P}_n$ , which are of the form

$$P(\mathbf{R}|\alpha, \boldsymbol{\rho}) = Z_n(\alpha, \boldsymbol{\rho})^{-1} \exp\left\{\frac{-\alpha}{n} d(\mathbf{R}, \boldsymbol{\rho})\right\} 1_{\mathcal{P}_n}(\mathbf{R}),$$

where  $\boldsymbol{\rho} \in \mathcal{P}_n$ ,  $\alpha$  is a positive scale parameter,  $Z_n(\alpha, \boldsymbol{\rho})$  is a proper normalizing constant, and  $1_S(\cdot)$  is the indicator function of the set  $S$ . If we assume that the  $N$  observed rankings  $\mathbf{R}_1, \dots, \mathbf{R}_N$  are conditionally independent given the latent ranking  $\boldsymbol{\rho}$ , and that each of them follows the Mallows model with parameters  $\boldsymbol{\rho}$  and  $\alpha$ , the likelihood takes the form

$$P(\mathbf{R}_1, \dots, \mathbf{R}_N|\alpha, \boldsymbol{\rho}) = Z_n(\alpha, \boldsymbol{\rho})^{-N} \exp\left(\frac{-\alpha}{n} \sum_{j=1}^N d(\mathbf{R}_j, \boldsymbol{\rho})\right) \prod_{j=1}^N \{1_{\mathcal{P}_n}(\mathbf{R}_j)\}. \quad (2)$$

### 2.1 Distance measures and normalizing constants

If the metric  $d(\cdot, \cdot)$  is right-invariant, i.e., invariant to an arbitrary relabeling of the items (Diaconis, 1988, p. 112), the normalizing constant is independent of  $\boldsymbol{\rho}$ , so we can write

$$Z_n(\alpha, \boldsymbol{\rho}) = Z_n(\alpha) = \sum_{\mathbf{R} \in \mathcal{P}_n} \exp\left(\frac{-\alpha}{n} d(\mathbf{R}, \mathbf{P})\right), \quad (3)$$

where  $\mathbf{P}$  denotes an arbitrary permutation in  $\mathcal{P}_n$ , say  $\mathbf{P} = (1, 2, \dots, n)$ . Since this is a sum over  $n!$  terms, analytic computation is in general intractable when  $n$  is larger than about 10.

The Kendall distance measures the minimum number of pairwise adjacent transpositions which convert  $\mathbf{R}$  into  $\mathbf{P}$ , and is given by the formula

$$d(\mathbf{R}, \mathbf{P}) = |\{(t, u) : t < u, (R_t > R_u \wedge P_t < P_u \vee R_t < R_u \wedge P_t > P_u)\}|,$$

where  $|\cdot|$  here denotes set cardinality. Its normalizing constant is given by  $Z_n(\alpha) = \prod_{i=1}^n \sum_{j=0}^{i-1} e^{-\alpha j/n}$ , which is a product over  $n$  terms, each being a summation over up to  $n$  terms (Mallows, 1957). Hence, in this special case, exact computation of  $Z_n(\alpha)$  is feasible also when  $n$  is large. For this reason, most applications of Mallows models have been restricted to Kendall distance (Lu and Boutilier, 2011; Meilă and Chen, 2010), except for cases in which the number of items is very small (Murphy and Martin, 2003).

However, other candidate metrics exist, and the choice of the most appropriate one from a statistical viewpoint depends on the particular application. Important right-invariant metrics are the *footrule distance*,  $d(\mathbf{R}, \mathbf{P}) = \sum_{i=1}^n |R_i - P_i|$ , and the *Spearman distance*  $d(\mathbf{R}, \mathbf{P}) = \sum_{i=1}^n (R_i - P_i)^2$ . Other examples are the Hamming distance, the Ulam distance and the Cayley distance (Marden, 1995, pp. 23-27). The computation of the normalizing constant in the Mallows model when using other distance measures than Kendall's is NP-complete, and no simple analytical form is known which avoids the summation over  $n!$  terms as in (3). Asymptotic approximations have been studied in Mukherjee (2013), which can be useful when the number of items  $n$  is very large. However, the applications we have in mind in this paper typically have at most a few hundred items  $n$ . Rather than relying on asymptotic approximations, we therefore develop an efficient importance sampling scheme which approximates  $Z_n(\alpha)$  to an arbitrary precision. Since it does not depend on  $\rho$ ,  $Z_n(\alpha)$  can be computed offline over a grid for  $\alpha$ , given  $n$ .

## 2.2 Prior distributions

The Bayesian framework allows incorporation of prior knowledge about the ranks  $\rho$  and the parameter  $\alpha$ . The choice of an appropriate prior distribution may vary from one application to the next. However, when no prior knowledge exists about  $\rho$ , an obvious choice is the (integrable) uniform distribution over  $\mathcal{P}_n$ , which we denote

$$\pi(\rho) = \frac{1}{n!} 1_{\mathcal{P}_n}(\rho). \quad (4)$$

Specifying the prior distribution for  $\alpha$ , on the other hand, can benefit from some reasoning. In the Mallows model we have terms of the form  $\exp\{(-\alpha/n)d(R_{ij}, \rho_j)\}$  contributing multiplicatively to the likelihood. To get some idea of what numerical values of  $\alpha$  would seem reasonable a priori, we can consider how likely it could be that the rank  $R_{ij}$  given by some assessor  $j$  to item  $A_i$  deviates from the rank  $\rho_i$  by at least  $n/2$ . An example of such a situation is when  $\rho_i$  is close to  $n/2$  (median), while  $R_{ij}$  is close to 1 (top) or  $n$  (bottom), or if  $\rho_i$  lies in the first quartile while  $R_{ij}$  lies in the third quartile. Using the footrule distance, this would correspond to  $d(R_{ij}, \rho_j) = n/2$ . We would then have the likelihood contribution  $\exp\{(-\alpha/n)d(R_{ij}, \rho_j)\} = \exp\{-\alpha/2\}$ . We can now specify our prior mean for  $\alpha$  such that it corresponds to our prior belief that an assessment could be off the mark by  $n/2$ . For example, with a mean of 10 our prior belief that this could happen is somewhat less than one percent. We represent this using the exponential distribution

$$\pi(\alpha) = \lambda \exp\{-\lambda\alpha\}, \quad (5)$$

with hyperparameter  $\lambda = 1/10$ . Since the footrule distance  $d_F$  and Kendall distance  $d_K$  are related by the inequality  $d_K \leq d_F \leq 2d_K$  (Diaconis and Graham, 1977, Th. 2), we use  $\lambda = 1/10$  when working with the Kendall distance as well.

For the Spearman distance, a similar reasoning would correspond to  $d(R_{ij}, \rho_j) = n^2/4$ , such that the likelihood contribution becomes  $\exp\{-\alpha n/4\}$ . A prior guess  $\alpha = 20/n$  now yields a contribution of about one percent, so we would here set  $\lambda = n/20$ .

We show in Sections S1.4 and S2.1 of the supplementary material that in some applications considered in this paper, the results are reasonably insensitive small changes in the hyperparameter  $\lambda$ .

### 2.3 Posterior distribution

Given prior distributions  $\pi(\boldsymbol{\rho})$  and  $\pi(\alpha)$ , the posterior distribution  $\boldsymbol{\rho}$  and  $\alpha$  is

$$P(\boldsymbol{\rho}, \alpha | \mathbf{R}_1, \dots, \mathbf{R}_N) \propto \frac{\pi(\boldsymbol{\rho}) \pi(\alpha)}{Z_n(\alpha)^N} \exp \left\{ -\frac{\alpha}{n} \sum_{j=1}^N d(\mathbf{R}_j, \boldsymbol{\rho}) \right\}. \quad (6)$$

In the next section we develop a Metropolis-Hastings algorithm for sampling from this distribution.

## 3 Metropolis-Hastings algorithm

In order to estimate  $\boldsymbol{\rho}$  and  $\alpha$  given  $\mathbf{R}_1, \dots, \mathbf{R}_N$ , using the posterior distribution (6), we iterate two steps. Given  $\alpha$ , our Metropolis-Hastings algorithm proposes a new permutation  $\boldsymbol{\rho}'$  given the current  $\boldsymbol{\rho}$  according to the distribution  $g(\boldsymbol{\rho}' | \boldsymbol{\rho})$ , and accepts it with probability

$$\min \left\{ 1, \frac{\exp \left( \frac{-\alpha}{n} \sum_{j=1}^N d(\mathbf{R}_j, \boldsymbol{\rho}') \right) \pi(\boldsymbol{\rho}') g(\boldsymbol{\rho} | \boldsymbol{\rho}')}{\exp \left( \frac{-\alpha}{n} \sum_{j=1}^N d(\mathbf{R}_j, \boldsymbol{\rho}) \right) \pi(\boldsymbol{\rho}) g(\boldsymbol{\rho}' | \boldsymbol{\rho})} \right\}. \quad (7)$$

Next, given  $\boldsymbol{\rho}$ , a proposal  $\alpha'$  given the current  $\alpha$  is drawn from the distribution  $g(\alpha' | \alpha)$ , and accepted with probability

$$\min \left\{ 1, \frac{Z_n(\alpha')^{-N} \exp \left\{ \frac{-\alpha'}{n} \sum_{j=1}^N d(\mathbf{R}_j, \boldsymbol{\rho}) \right\} \pi(\alpha') g(\alpha | \alpha')}{Z_n(\alpha)^{-N} \exp \left\{ \frac{-\alpha}{n} \sum_{j=1}^N d(\mathbf{R}_j, \boldsymbol{\rho}) \right\} \pi(\alpha) g(\alpha' | \alpha)} \right\}. \quad (8)$$

To ensure that the proposals  $\boldsymbol{\rho}'$  have a reasonable acceptance ratio, our choice of  $g(\boldsymbol{\rho}' | \boldsymbol{\rho})$  imposes small perturbations of the elements of  $\boldsymbol{\rho}$  while keeping  $\boldsymbol{\rho}' \in \mathcal{P}_n$ . This *leap-and-shift* distribution is described in Section 3.1. For  $\alpha'$ , we simply set  $g(\alpha' | \alpha) = \mathcal{N}(\alpha, \sigma^2)$ , where the variance  $\sigma^2$  is tuned to give a reasonable acceptance ratio. Both proposal distribution are symmetric, so the Hastings corrections in (7) and (8) cancel.

Next, we need an approximation of  $Z_n(\alpha)$  for all  $\alpha$  values which the MCMC algorithm might propose. The latter problem has been a major obstacle for the use of Mallows models with other metrics than the Kendall distance. Our solution to this problem is described in Section 3.2. The resulting algorithms were implemented in R callable C++ code using the Rcpp package (Eddelbuettel and François, 2011; Eddelbuettel, 2013).

### 3.1 Leap-and-shift proposal distribution

We now give an intuitive description of the proposal distribution for  $\boldsymbol{\rho}$ , deferring the mathematical details to Appendix A.1.

Let  $\boldsymbol{\rho}$  be the current rank vector, and fix some  $L \in \{1, \dots, \lceil n/2 \rceil\}$ . Draw uniformly a random integer  $U = u$  between 1 and  $n$ , corresponding to an item  $A_u$  with current rank  $\rho_u$ . Define

$$\mathcal{S} = \begin{cases} \{\rho_u - L, \dots, \rho_u + L\} \setminus \{\rho_u\}, & \text{if } L + 1 \leq \rho_u \leq n - L \\ \{1, \dots, 2L\} \setminus \{\rho_u\}, & \text{if } \rho_u \leq L \\ \{n - 2L + 1, \dots, n\} \setminus \{\rho_u\}, & \text{if } \rho_u \geq n - L + 1, \end{cases}$$

and draw a new rank  $\rho'_u$  uniformly on the set  $\mathcal{S}$ . Now define the new vector  $\boldsymbol{\rho}'$  with elements  $\rho'_i = \rho'_u$  if  $i = u$  and  $\rho'_i = \rho_i$  otherwise. This completes the *leap* step.

After the leap step,  $\boldsymbol{\rho}'$  is not a proper rank vector, since there exist two indices  $i \neq j$  such that  $\rho'_i = \rho'_j$ . Hence, we need to *shift* the elements whose ranks are between  $\rho_u$  and  $\rho'_u$  by one, to account for the leap. Let  $\Delta = \rho'_u - \rho_u$  denote the size of the leap, and let

$$\rho'_i \leftarrow \begin{cases} \rho_i - 1 & \text{for } i : \rho_u < \rho_i \leq \rho'_u, & \text{if } \Delta > 0 \\ \rho_i + 1 & \text{for } i : \rho'_u \leq \rho_i < \rho_u, & \text{if } \Delta < 0. \end{cases}$$

This yields a proposal  $\boldsymbol{\rho}' \in \mathcal{P}_n$  which is a local perturbation of the current value  $\boldsymbol{\rho}$ . In fact, if  $d(\cdot, \cdot)$  is taken to be the Ulam distance, we have  $d(\boldsymbol{\rho}', \boldsymbol{\rho}) = 1$  (Marden, 1995, pp. 26-27). The parameter  $L$  can be used to tune the acceptance ratio. In Appendix A.1 we write an explicit formula for this proposal distribution  $g(\boldsymbol{\rho}'|\boldsymbol{\rho})$ .

### 3.2 Computing $Z_n(\alpha)$ by importance sampling

To sample  $\alpha$  for fixed ranks  $\boldsymbol{\rho}$ , the Metropolis-Hastings ratio (8) has to be computed for the proposal  $\alpha'$  given the current  $\alpha$ . This ratio involves  $Z_n(\alpha)$ , which is not feasible to compute other than for very small  $n$ . We thus propose an importance sampling algorithm which yields an estimate  $\hat{Z}_n(\alpha)$ . Since  $Z_n(\alpha)$  does not depend on  $\boldsymbol{\rho}$ , the approximation can be done offline for a set of discrete  $\alpha$  values, and interpolated to yield an estimate over a continuous range. For each  $\alpha'$  proposed in the MCMC algorithm, it is then sufficient to look up the value  $\hat{Z}_n(\alpha')$  in our stored estimate.

The complete algorithm is described in Appendix A.2. The basic idea is to approximate (3) by summing only  $K \ll n!$  ranks  $\mathbf{R}$  sampled at random in  $\mathcal{P}_n$ , where the probability of drawing each  $\mathbf{R}$  is close to its weight in the sum,  $\exp((-\alpha/n)d(\mathbf{R}, \mathbf{P}))$ . Dividing each term by the probability of its rank  $\mathbf{R}$ , and then taking the mean, we obtain an unbiased estimator of  $Z_n(\alpha)$ . The goodness of this approximation depends on the choice of the sampling distribution. We use a directional pseudo-likelihood from which it is easy to sequentially sample the components of  $\mathbf{R}$ , obtained by approximating the joint likelihood (2) with the chain multiplication rule. The mathematical details can be found in Appendix A.1, and we show in Section S5 of the supplement that very good estimates are obtained with  $K \ll n!$  samples.

## 4 The potato experiment

To illustrate the method, we first consider an experiment where the true value of  $\boldsymbol{\rho}$  is known. We bought a bag of potatoes, with a total weight of approximately 1.5 kilograms. The potatoes were picked out from the bag one at a time, without any form of selection based on size or otherwise, and then marked by letter codes A, B, ... It turned out that there were  $n = 20$  potatoes in the bag, so the last potato was marked with the letter T. We then spread the potatoes on a table, and asked 12 of our colleagues and students to rank the potatoes according to their weight twice: first, by *visual inspection*, being only allowed to look at the potatoes on the table and order them in the desired way without lifting them. Later on, he/she was allowed to feel the weight of the potatoes by holding them, and to change the ranking from the first assessment as needed. The assessors acted independently. Figures S. and S. in the supplement show photos of the potatoes and of the visual inspection experiment. In our notation, we label the potatoes  $A_1, A_2, \dots, A_{20}$ , such that  $A_1$  corresponds to potato A,  $A_2$  corresponds to potato B, and so on. We afterwards measured the weights of all individual potatoes, thus deriving the true  $\boldsymbol{\rho}$ .

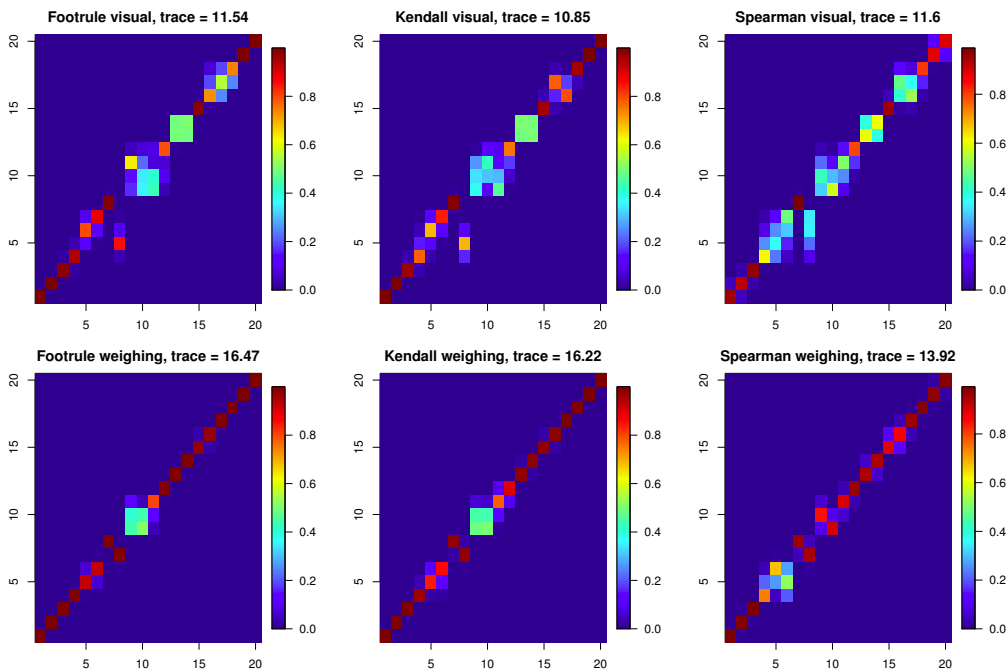


Figure 1: Heat plots of the latent ranks (vertical axis) versus the true rank (horizontal axis) for the potato experiment. The trace represents the posterior expectation of the number of correctly ranked potatoes.

Based on the discussion about prior distributions in Section 2.2, we found it reasonable to assume a prior probability of about one percent that an assessor would rank a potato about  $n/2$  away from its true value. We thus chose the exponential distribution with rate  $\lambda = 1/10$  as our prior distribution when using the footrule and Kendall distance, and the exponential distribution with rate  $\lambda = n/20$  when using the Spearman distance. All results are based on one million iterations of the Metropolis-Hastings algorithm after burn-in.

## 4.1 Results

Figure 1 shows heat plots of latent ranks on the vertical scale versus the true ranks on the horizontal scale. In each plot, the matrix trace represents posterior expectation of the number of correctly ranked potatoes,  $\sum_{i=1}^n 1_{\{\hat{\rho}_i = \rho_i\}} P(\hat{\rho}_i = \rho_i | \text{data})$ . In the visual inspection experiment, the Mallows model with Spearman distance had the largest trace, closely followed by the model with the footrule distance, while the model with the Kendall distance had the smallest. On the other hand, in the weighing experiment, the Mallows model with the footrule distance performed slightly better than with Kendall distance, and both were much better than the Spearman distance.

The results from the heat plots in Figure 1 are supported by the plots in Figure 2, which show posterior CDFs for the total footrule distance between the latent and the true ranks. The CDF for the total Kendall or Spearman distance between the latent and the true ranks gave practically equal results, and the corresponding plots are shown in Figure S3 of the supplementary material. For the visual data, the latent ranks from the Mallows model with the Spearman distance were

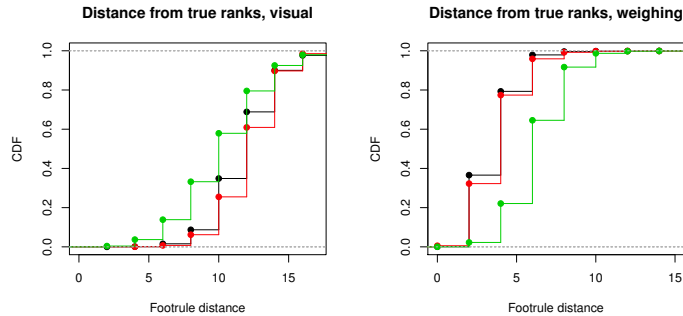


Figure 2: The posterior distributions, expressed in terms of the CDFs for the total distance between the latent and true ranks when measured by the footrule distance. The blue curves represent the posterior distributions for the latent ranks in the Mallows model with the footrule distance, the red curves with the Kendall distance, and the green curves with the Spearman distance.

closest to the true ranks. Similarly, in the weighing experiment, the latent ranks from the Mallows model with the footrule distance and the Kendall distance had a very similar distance to the true ranks, while the latent ranks from the Mallows model with the Spearman distance were further away from the true ranks in this experiment. We see from the heat plots that the middle range potatoes are assessed less accurately than those at the extremes. This is especially the case in the visual inspection experiment. Figures S4 and S5 in the supplementary material illustrate this further, showing posterior histograms of the latent rank for the heaviest potato, the two potatoes closest to the median weight, and the lightest potato.

One might have expected that the Mallows model with the footrule distance would yield latent ranks which are closer to the true ranks when measured by the footrule distance, and that a similar relationship would hold for the Kendall and the Spearman distances, but this was not the case here. The different distance measures perform varyingly in the different situations, but overall the Mallows model with the footrule distance seems to be the best in order to maximize the expected number of correctly ranked potatoes in Figure 1.

## 5 Partially ranked data

A situation frequently arising in applications is that only a subset of the items have been ranked. Ranks can be missing at random, or the assessors may only have ranked, say, the top-five items. These types of situations can be handled fairly easily in our Bayesian framework, by applying data augmentation techniques (Tanner and Wong, 1987).

Assume that each assessor  $j$  has ranked the items in  $\mathcal{A}_j \subseteq \{A_1, A_2, \dots, A_n\}$ . We define the elements of the rank vector for assessor  $j$  as  $R_{ij} = \mathbf{X}_j^{-1}(A_i)$  if  $A_i \in \mathcal{A}_j$ , and  $R_{ij} = \star$  otherwise, for  $i = 1, \dots, n$ ,  $j = 1, \dots, N$ . Our goal is to sample from the posterior distribution

$$P(\alpha, \boldsymbol{\rho} | \mathbf{R}_1, \dots, \mathbf{R}_N) = \sum_{\tilde{\mathbf{R}}_1 \in \mathcal{S}_1} \cdots \sum_{\tilde{\mathbf{R}}_N \in \mathcal{S}_N} P(\alpha, \boldsymbol{\rho} | \tilde{\mathbf{R}}_1, \dots, \tilde{\mathbf{R}}_N) P(\tilde{\mathbf{R}}_1, \dots, \tilde{\mathbf{R}}_N | \mathbf{R}_1, \dots, \mathbf{R}_N), \quad (9)$$

where  $\mathcal{S}_j$  is the set of allowable 'fill-ins' of the missing ranks in  $\mathbf{R}_j$ ,

$$\mathcal{S}_j = \left\{ \tilde{\mathbf{R}}_j \in \mathcal{P}_n : \tilde{R}_{ij} = \mathbf{X}_j^{-1}(A_i) \text{ if } A_i \in \mathcal{A}_j \right\}, j = 1, \dots, n.$$

Here,  $\tilde{\mathbf{R}}_1, \dots, \tilde{\mathbf{R}}_N$  are augmented rank vectors chosen to be consistent with the partial observations. The term  $P(\alpha, \boldsymbol{\rho} | \tilde{\mathbf{R}}_1, \dots, \tilde{\mathbf{R}}_N)$  in (9) is the posterior joint distribution for  $\alpha$  and  $\boldsymbol{\rho}$  given the augmented data, and we can sample from it using the techniques developed in the previous sections. Furthermore, by fixing the observed ranks  $\mathbf{R}_1, \dots, \mathbf{R}_N$  in the full likelihood (2), we see that

$$P(\tilde{\mathbf{R}}_1, \dots, \tilde{\mathbf{R}}_N | \alpha, \boldsymbol{\rho}, \mathbf{R}_1, \dots, \mathbf{R}_N) = \frac{1_{\mathcal{S}_j}(\tilde{\mathbf{R}}_j)}{Z_n(\alpha)^N} \exp\left(\frac{-\alpha}{n} \sum_{j=1}^N d(\tilde{\mathbf{R}}_j, \boldsymbol{\rho})\right). \quad (10)$$

We can thus alternate between sampling the augmented ranks given the current values of  $\alpha$  and  $\boldsymbol{\rho}$  from (10), and given the current value of the augmented ranks, sampling  $\alpha$  and  $\boldsymbol{\rho}$  from  $P(\alpha, \boldsymbol{\rho} | \tilde{\mathbf{R}}_1, \dots, \tilde{\mathbf{R}}_N)$ . At convergence, this yields samples from the joint distribution  $P(\alpha, \boldsymbol{\rho}, \tilde{\mathbf{R}}_1, \dots, \tilde{\mathbf{R}}_N | \mathbf{R}_1, \dots, \mathbf{R}_N)$ .

Sampling  $\alpha$  and  $\boldsymbol{\rho}$  given an augmented data set is done using the Metropolis-Hastings algorithm as described earlier for complete data. In order to propose new values of the unobserved ranks for assessor  $j$ , we use a uniform distribution on  $\mathcal{S}_j$ , and accept with probability given by the Metropolis-Hastings ratio derived from (10).

## 5.1 Top-5 estimation in the potato experiment

In many applications, the full ranking of all the items is not of main interest, and one may rather aim at finding the top- $t$  items, for some small number  $t$ . In these cases, it is important to consider how many top ranks each assessor should identify. For example, if we are interested in identifying the top-5, should we then ask the assessors to give full rankings, to rank only the top-5, or should we decide some other number of top items? Collecting complete ranks is more demanding than asking for only the top items, so these types of questions are important in planning of experiments. We investigate this in the case of top-10 and top-5 datasets for our potato experiment, by ignoring ranks above 10 or 5, respectively. We focus on the weighing experiment here, and present similar results for the visual inspection experiment in Section S1.3 of the supplementary material. In these examples, we still used an exponential prior distribution with  $\lambda = 1/10$  for the footrule and Kendall distance, and  $\lambda = n/20$  for the Spearman distance. 12 out of 20 potatoes had been ranked among the top-10 by at least one assessor, and were kept in the data set, resulting in 2 missing ranks for each assessor. The remaining 8 potatoes were not included in the analysis. Similarly, 8 out of 20 potatoes were ranked as top-5 by at least one assessor, so we kept these in the data set, resulting in three missing ranks per assessor.

Figure 3 shows heat plots of the estimated five heaviest potatoes, corresponding to the lower left corners in Figure 1. The top row shows the results when only the top-5 potatoes were provided by each assessor, and the bottom row when the top-10 potatoes were identified. In this case, using only the top-5 data seems to give a higher precision in the top-5 estimation for all three models, although the difference is clear only in the case of the Spearman distance model. This might seem counterintuitive, since the results got worse when more data were gathered. However, when using the top-10 ranks from each assessor, 12 of the potatoes were ranked and used in the model, compared to 8 potatoes when using the top-5 ranks. Thus, when using the top-10 ranks, there were four additional potatoes in the model which could get values between 1 and 5, thereby explaining why the accuracy is lower in this case. We also see that the model

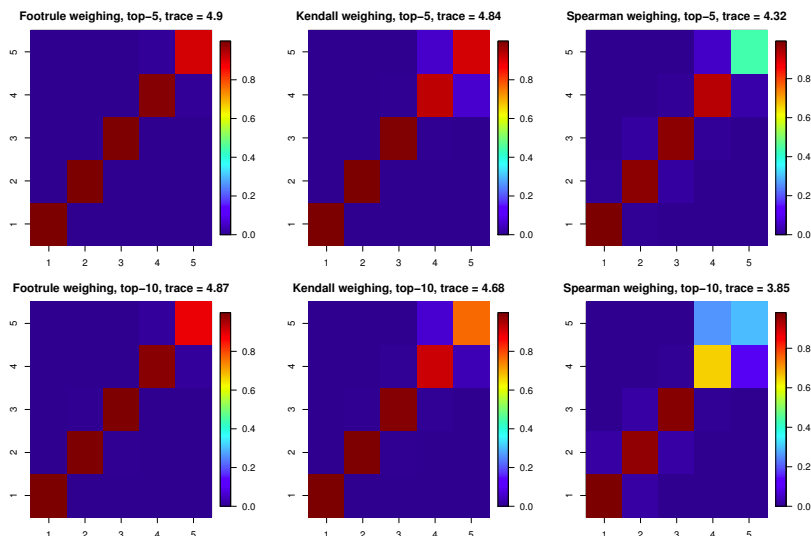


Figure 3: Estimation of the five heaviest potatoes when using only the five heaviest potatoes (top), and when using only the ten heaviest potatoes (bottom).

with the footrule distance provided the best estimates in this case, closely followed by the model with the Kendall distance.

## 6 Ordered subsets and pairwise comparisons

In many situations, the data take the form of comparisons between items, rather than a complete ranking. An important case arises when the assessors perform multiple pairwise comparisons, yielding a union of linear orderings. For the Mallows model with the Kendall distance, Lu and Boutilier (2011) have studied the case of pairwise comparisons. Our data augmentation scheme, outlined in the previous section, can be modified to also handle these types of situations, with the added flexibility that any right-invariant distance measure can be used.

To give a simple example of paired comparisons, an assessor  $j$  could have stated the preferences  $\mathcal{B}_j = \{A_1 \prec A_2, A_2 \prec A_5, A_4 \prec A_5\}$ , for each assessor  $j$ . Here  $A_r \prec A_s$ , for some  $r \neq s$ , means that  $A_s$  is preferred to  $A_r$ . Hence,  $A_s$  will have a *lower* rank than  $A_r$ . We denote by  $\mathcal{A}_j$  the set of items constrained by assessor  $j$ . In this case, we would have  $\mathcal{A}_j = \{A_1, A_2, A_4, A_5\}$ . This problem differs from the one studied in Section 5 since now the constrained items are not necessarily fixed to a given rank. Hence, in order to develop an efficient MCMC algorithm, we need to propose augmented ranks which obey the partial ordering constraints given by the assessor. Otherwise, a large number of proposals would be rejected. We assume that the pairwise orderings in  $\mathcal{B}_j$  are mutually compatible, and then denote by  $\text{tc}(\mathcal{B}_j)$  the transitive closure of  $\mathcal{B}_j$ , including all the pairwise orderings of the elements in  $\mathcal{A}_j$  coherent with the pairwise orderings in  $\mathcal{B}_j$ . For the pairwise orderings given in  $\mathcal{B}_j$  above, we find  $\text{tc}(\mathcal{B}_j) = \mathcal{B}_j \cup \{A_1 \prec A_5\}$ . For the case of ordered subsets of items, the transitive closure is simply the single set of pairwise preferences compatible with the ordering, e.g.,  $\{A_1 \prec A_2 \prec A_5\}$  would yield  $\text{tc}(\mathcal{B}_j) = \{A_1 \prec A_2, A_2 \prec A_5\}$ .

The leap-and-shift algorithm requires a simple adjustment in order to propose augmented ranks which are consistent with the partial ordering constraints. First, suppose that from the last step of the MCMC algorithm we have a full rank vector  $\hat{\mathbf{R}}_j$  for assessor  $j$  which is consistent

with  $\text{tc}(\mathcal{P}_j)$ . Now draw a random number  $u$  uniformly from the set  $\{1, \dots, n\}$ . If  $A_u \in \mathcal{A}_j$ , i.e., if item  $A_u$  is among the constrained items, then define

$$l_j = \max \left\{ \tilde{R}_{kj} : A_k \in \mathcal{A}_j, k \neq u, (A_k \succ A_u) \in \text{tc}(\mathcal{B}_j) \right\},$$

with the convention that  $l_j = 0$  if the set is empty, and define

$$r_j = \min \left\{ \tilde{R}_{kj} : A_k \in \mathcal{A}_j, k \neq u, (A_k \prec A_u) \in \text{tc}(\mathcal{B}_j) \right\},$$

with the convention that  $r_j = n + 1$  if the set is empty. Now complete the *leap* step by drawing a new proposal  $\tilde{R}'_{uj}$  uniformly from the set  $\{l_j + 1, \dots, r_j - 1\}$ . Otherwise, if  $A_u \notin \mathcal{A}_j$ , we complete the *leap* step by drawing  $\tilde{R}'_{uj}$  uniformly over  $\{1, \dots, n\}$ . Next, we proceed with the *shift* step in exactly the same manner as described earlier.

## 6.1 A Premier League season

The Premier League of the English football league system consists of 20 teams, which all play one home game and one away game againsts all the other teams each season, giving a total of 38 matchdays. In the final league table, a win gives 3 points, draw gives 1 point, and loss gives 0 points. In the season of 2010/2011, Manchester United won ahead of Chelsea and Manchester City, while Birmingham, Blackpool, and West Ham ended 18th, 19th, and 20th, respectively.

The Mallows model can give an alternative ranking of the teams, by considering each matchday as an assessor. Each game not ending in a draw counts as a pairwise preference, such that each of the 38 matchdays gives a maximum of 10 pairwise preferences. Excluding the draws in this way, we considerably simplified the modeling of game outcomes. Our aim is to illustrate how the Mallows model for pairwise preferences can be used to obtain an alternative to the official league table. A predictive model for betting would likely take into account a large number of other factors which we have not included, like home game vs. away game, goal differences, recent performances, injuries, etc. For an analysis of team strengths in English football between 1888 and 2012, see Baker and McHale (2014).

We obtained results from the whole Premier League season of 2010/2011, and generated the transitive closure for each matchday using the R packages `sets` (Meyer and Hornik, 2009) and `relations` (Meyer and Hornik, 2014). The Bayesian Mallows model for pairwise preferences was then run, with a prior for  $\alpha$  which was uniform over the positive half line, and using the footrule distance.

In order to create a summary of the joint posterior distribution for the ranks of all teams, we first identified the team with highest marginal posterior probability of having rank 1, and put this team on top of the list. Next, among the remaining teams, we chose the one with the highest marginal posterior probability of having rank 1 or 2, and placed this team second on the list. This procedure was continued until all the 20 teams had been ranked. Table 1 shows the official results of the Premier League in the left panel, and the teams arranged by our ranking procedure in the right panel. The numbers in the CP column denote the cumulative posterior probability of having a rank corresponding to the team's position in the list or higher. The numbers in parentheses show the 90 % highest posterior density intervals (HPDI) for the ranks of each team. Overall, Table 1 shows that the results derived by applying the Mallows model agree very well with the official league table. For example, the five highest ranks are given in both tables to the same teams in the same order, and the same six teams occupy the last positions from 15 to 20. On the other hand, the last column of Table 1 shows that the HPDI are very wide, apparently because there is considerable variability in the outcomes from individual games, but also because the data are fairly sparse, as each pair of teams meet only twice per season.

Table 1: Left: official Premier League table for the season 2010/11, with total score (Pts.) and goal differences (GD). Right: and the teams arranged by their cumulative probability (CP) in the Mallows model.

Official League Table				Mallows Footrule Table			
Team	Pts.	GD	Team	CP	90 % HPDI		
1	Man. United	80	+41	1	Man. United	0.31	(1,5)
2	Chelsea	71	+36	2	Chelsea	0.31	(1,8)
3	Man. City	71	+27	3	Man. City	0.45	(1,8)
4	Arsenal	68	+29	4	Arsenal	0.58	(1,8)
5	Tottenham	62	+9	5	Tottenham	0.61	(1,9)
6	Liverpool	58	+15	6	Everton	0.48	(1,13)
7	Everton	54	+6	7	Liverpool	0.51	(1,13)
8	Fulham	49	+6	8	Fulham	0.45	(2,16)
9	Aston Villa	48	-11	9	Aston Villa	0.36	(4,18)
10	Sunderland	47	-11	10	West Bromwich	0.39	(5,19)
11	West Bromwich	47	-15	11	Bolton	0.42	(6,19)
12	Newcastle	46	-1	12	Newcastle	0.50	(7,20)
13	Stoke City	46	-2	13	Sunderland	0.57	(7,20)
14	Bolton	46	-4	14	Stoke City	0.62	(8,20)
15	Blackburn	43	-13	15	Blackburn	0.61	(9,20)
16	Wigan	42	-21	16	Wigan	0.67	(8,20)
17	Wolverhampton	40	-20	17	Birmingham	0.65	(10,20)
18	Birmingham	39	-21	18	Blackpool	0.75	(10,20)
19	Blackpool	39	-23	19	Wolverhampton	0.87	(11,20)
20	West Ham	33	-27	20	West Ham	1.00	(13,20)

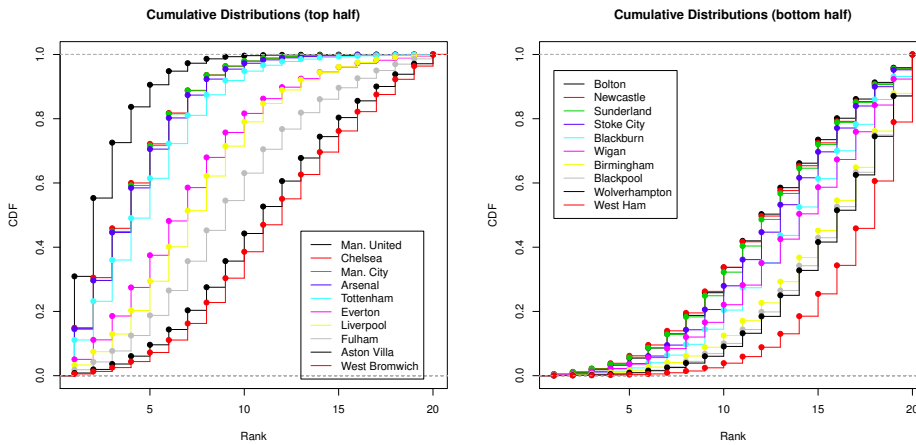


Figure 4: Posterior cumulative distribution functions for the ranks of the teams in the Premier League in the 2010/11 season.

To complement the resulting high degree of uncertainty in the posteriors of the individual rankings, Figure 4 gives an alternative view, by displaying the posterior CDFs for the rankings of all twenty teams. Although some of the curves are overlapping, they also reveal perfect stochastic orderings between most of the teams. Studying the curves carefully shows that Manchester United stochastically dominates all other teams, while West Ham is stochastically dominated by all other teams. On the other hand, some teams ranked very closely, like Manchester City and Chelsea, or Bolton and Newcastle, are not stochastically ordered, meaning that their curves in Figure 4 overlap. Table S1 in the supplementary material shows an indicator matrix for all the stochastic orderings deduced from Figure 4.

## 7 Clustering the assessors via mixtures

The models considered so far are based on the assumption that there exists a unique true ranking of the items with respect to the given feature. This assumption is clearly met if there is an underlying, at least ordinal, measurement scale which determines the rankings, such as grams in the potato experiment. However, it may no longer be adequate in situations where the rankings are more subjective, e.g. arise from inquiries concerning consumer preferences. More likely, a heterogeneous population of respondents or assessors, can be usefully divided into more homogeneous segments or clusters, each expressing a typical profile in the preferences that are expressed.

We propose to handle this issue by using a hierarchical Bayesian mixture of Mallows models, where each component of the mixture is thought to correspond to a relatively more homogeneous sub-population of the whole. Mixtures of distance-based models have been previously used to analyze rank data from heterogeneous populations in a frequentist framework (Lu and Boutilier, 2011; Busse et al., 2007; Murphy and Martin, 2003), while Bayesian approaches have been limited to the cases of the Plackett-Luce (Caron et al., 2014) and of the generalized Mallows models, which are based on the Kendall distance (Meilă and Chen, 2010).

Suppose that the  $N$  assessors have been selected from an heterogeneous population with  $C \geq 1$  components or clusters. Let the variables  $z_1, \dots, z_N \in \{1, \dots, C\}$  assign each assessor to one of these sub-populations. The assessments within each cluster  $c$ ,  $c = 1, \dots, C$ , are described by a Mallows model with scale and location parameters  $\alpha_c$  and  $\boldsymbol{\rho}_c$ , respectively. Then, assuming conditional independence across the clusters, the augmented data formulation of the likelihood for the observed rankings  $\mathbf{R}_1, \dots, \mathbf{R}_N$  is given by

$$P(\mathbf{R}_1, \dots, \mathbf{R}_N | \boldsymbol{\rho}_1, \dots, \boldsymbol{\rho}_C; \alpha_1, \dots, \alpha_C; z_1, \dots, z_N) = \prod_{j=1}^N \frac{1_{\mathcal{P}_n}(\mathbf{R}_j)}{Z_n(\alpha_{z_j})} \exp\left(\frac{-\alpha_{z_j}}{n} d(\mathbf{R}_j, \boldsymbol{\rho}_{z_j})\right). \quad (11)$$

The location parameters  $\boldsymbol{\rho}_1, \dots, \boldsymbol{\rho}_C$  are assumed to be a priori independent, and they are all assigned the same uniform prior given in (4). The prior for the scale parameters  $\alpha_1, \dots, \alpha_C$  follows marginally (5), with the additional constraint needed for cluster identifiability. Indeed, non-identifiability problems (referred to as label switching in Stephens (2000); Celeux et al. (2000)) are a well known difficulty in clustering, often solved by imposing a constraint on some of the parameters (Jasra et al., 2005). Here we specify a prior for the scale parameters by

$$\pi(\alpha_1, \dots, \alpha_C) \propto \lambda^C \cdot \exp\left\{-\lambda \sum_{c=1}^C \alpha_c\right\} \cdot 1_{\{\alpha_1 < \dots < \alpha_C\}}(\alpha_1, \dots, \alpha_C). \quad (12)$$

Let us then assume that the cluster labels are assigned independently according to the prior

$$P(z_1, \dots, z_N | \tau_1, \dots, \tau_C) = \prod_{j=1}^N \tau_{z_j}, \quad (13)$$

where  $\tau_c$  is the probability that an assessor belongs to the  $c$ -th sub-population;  $\tau_c \geq 0$ ,  $c = 1, \dots, C$  and  $\sum_{c=1}^C \tau_c = 1$ . We complete the model specification by assigning to  $\tau_1, \dots, \tau_C$  the standard symmetric Dirichlet prior

$$\pi(\tau_1, \dots, \tau_C) = \frac{\Gamma(\psi C)}{\Gamma(\psi)^C} \prod_{c=1}^C \tau_c^{\psi-1}, \quad (14)$$

which is parametrized by a single scalar value  $\psi$ , called the concentration parameter.

Combining (11)-(14), the posterior distribution for the mixture model is given by

$$\begin{aligned} &P(\boldsymbol{\rho}_1, \dots, \boldsymbol{\rho}_C; \alpha_1, \dots, \alpha_C; \tau_1, \dots, \tau_C; z_1, \dots, z_N | \mathbf{R}_1, \dots, \mathbf{R}_N) \\ &\propto P(\mathbf{R}_1, \dots, \mathbf{R}_N | \boldsymbol{\rho}_1, \dots, \boldsymbol{\rho}_C; \alpha_1, \dots, \alpha_C; z_1, \dots, z_N) \\ &\cdot P(\boldsymbol{\rho}_1, \dots, \boldsymbol{\rho}_C) \cdot P(z_1, \dots, z_N | \tau_1, \dots, \tau_C) \cdot P(\tau_1, \dots, \tau_C) \cdot P(\alpha_1, \dots, \alpha_C) \end{aligned} \quad (15)$$

To obtain samples from the posterior (15) a proper MCMC scheme is implemented, whose details are given in Appendix A.3. We have assumed so far that the number  $C$  of sub-populations forming the mixture is known. However, in most situations there is no firm a priori knowledge about the number of sub-populations present in the sample. We handle the choice of  $C$  by inspecting the within cluster sum of squares distances of observed ranks from the corresponding latent cluster center.

## 7.1 Analysis of sushi data

This dataset consists of sushi preferences surveyed across Japan. These preference data are collected by a questionnaire survey described in Kamishima (2003), and they can be downloaded from <http://www.kamishima.net/sushi/>.  $N = 5000$  people (assessors) were interviewed, each giving his/her complete ranking of  $n = 10$  sushi variants (items): *ebi* (shrimp), *anago* (sea eel), *maguro* (tuna), *ika* (squid), *uni* (sea urchin), *sake* (salmon roe), *tamago* (egg), *toro* (fatty tuna), *tekka-maki* (tuna roll), and *kappa-maki* (cucumber roll). This dataset has been previously analyzed in Lu and Boutilier (2011) as a benchmark for testing clustering procedures for ranked data. Historically, cultural differences among Japanese regions (e.g., between the Mikado noble culture in the west and the Shogun/Samurai warriors' culture in the east) have influenced the preference patterns of food. Therefore, we expect the assessors to be clustered around a few common preferences, possibly characterizing regional/age groups.

We analysed the sushi data using mixtures of Mallows models, applying both the footrule and Spearman distances, and exploring systematically all values of  $C$  from 1 to 10. We show here the results obtained with the footrule distance, leaving those based on the Spearman distance to the supplementary material. We fixed the value of the hyperparameter of the prior for  $\boldsymbol{\tau}$  at  $\psi = 2$ , thus favouring high-entropy distributions. The MCMC was run for one million iterations, and the first 100000 were discarded as burn-in. Convergence issues are addressed in the supplementary material.

In order to find an appropriate value for  $C$ , from a random thinned selection of MCMC samples after burn-in we computed the footrule distances between each currently estimated cluster center (latent rank) and the preference data of each assessor assigned to that cluster.

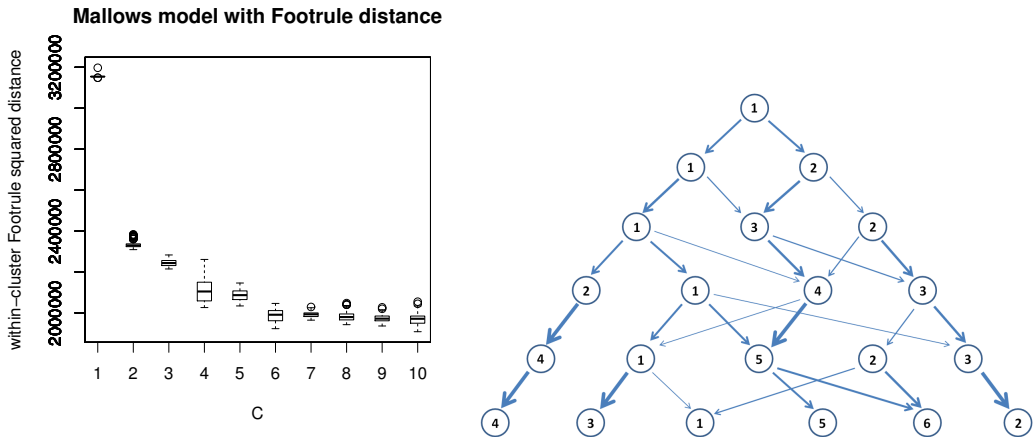


Figure 5: Cluster analysis of the sushi dataset when applying Mallows mixture models with the footrule distance. Left: boxplots of the posterior distributions of the within-cluster SSE’s for different choices of  $C$ . Right: the arrows in the graph represent the flow of assessors moving from a cluster to another when  $C$  is increased, according to the MAP cluster assignment for each  $C$ . The thickness of arrows is approximately proportional to the volume of the flow.

The sum of squares of such within-cluster distances, across all assessors and cluster centers, is viewed as a Sum-of-Squares Error (SSE), and its posterior distribution was used for choosing an appropriate value for  $C$ .

The boxplots of the marginal posterior distributions of the consequent within-cluster SSE’s for the models with  $C = 1, \dots, 10$  are shown in Figure 5 (left panel). The SSE obtained for  $C = 1$  is the total sum of squares from a common center. Looking at this figure we find an elbow at  $C = 6$ , after which the SSE values stabilize to essentially the same level. Thus our comments below are concerned with this value of  $C$ .

Table 2 reports, for each cluster, the maximum a posteriori (MAP) estimates for  $\tau$  and  $\alpha$ , together with their 95% highest posterior density intervals (HPD), and the sushi items arranged as in the MAP estimate for cluster centers. Interestingly, there is a quite good agreement between the clustering results obtained here by applying the Mallows models mixture with the footrule distance, and those established for  $C = 6$  in Lu and Boutilier (2011). Note that smaller values of  $\alpha$  do not correspond in general to bigger clusters, thus indicating an overall low uncertainty around the estimated rankings and a robustness of the classification.

In order to get a better understanding of the differences between the clustering structures obtained with different values of  $C$ , Figure 5 (right panel) shows the shift of assignment of assessors between clusters when one new cluster is added to the mixture. The figure is based on the MAP estimates of cluster assignments for increasing  $C$ , ranging from 1 to 6, obtained from 6 independent MCMC runs. The thickness of an arrow represents the proportion of assessors in the cluster who move along that route, and only flows bigger than 5% are displayed for ease of representation. We observe that the clusters evolve across generations of  $C$  mostly by either splitting into two, or by consistently forming the same cluster in the next generation, providing evidence of a reasonable degree of stability in the cluster memberships for different values of  $C$ . It also happens quite often that two or three arrows merge, i.e., a node has at least two parents in the graph, corresponding to a situation in which a new cluster center attracts many assessors from their previous assignments. This is not surprising, since we do not have any constraint on

Table 2: Results obtained from the cluster analysis with the Mallows mixture model with footrule distance, for  $C = 6$ : sushi items arranged according to the MAP estimates of the cluster centers, together with the corresponding MAP estimates for  $\tau$  and  $\alpha$  (with 95% HPD intervals).

Cluster	$c = 1$	$c = 2$	$c = 3$
$\tau_c$	19.08% (17.26%,20.51%)	8.97% (7.31%,10.43%)	24.03% (21.94%,25.88%)
$\alpha_c$	1.56 (1.52,1.60)	1.82 (1.71,2.0)	2.9 (2.76,3.12)
	sea urchin fatty tuna sea eel salmon roe shrimp tuna squid tuna roll egg cucumber roll	fatty tuna tuna sea urchin salmon roe tuna roll squid shrimp sea eel egg cucumber roll	fatty tuna tuna sea eel shrimp tuna roll squid egg cucumber roll salmon roe sea urchin
Cluster	$c = 4$	$c = 5$	$c = 6$
$\tau_c$	5.42% (4.55%,6.11%)	4.21% (3.95%,5.03%)	38.27% (36.14%,40.77%)
$\alpha_c$	2.91 (2.78,3.15)	3.11 (2.97,3.34)	3.92 (3.77,4.15)
	shrimp egg squid sea eel cucumber roll salmon roe tuna roll fatty tuna tuna sea urchin	salmon roe fatty tuna tuna tuna roll egg shrimp squid cucumber roll sea eel sea urchin	fatty tuna sea urchin salmon roe tuna shrimp sea eel tuna roll squid egg cucumber roll

clusters being nested across generations.

## 8 Modeling of time-dependent ranks

There are many situations in which the true ranks vary over time. Regenwetter et al. (1999) studies how voters' rankings of the three major candidates evolved prior to the 1992 US presidential elections, and estimated the impact of external information (campaigning) using a mathematical theory developed in Falmagne (1996). Caron and Teh (2012) considers the New York Times best-seller books over a period of 4 years, and modeled them with a Plackett-Luce model. We provide here another example, where we study high school students' performances in mathematics over a 4-year period.

Our framework for modeling time-dependent ranks with the Mallows model is based on dynamic Bayesian networks (Koller and Friedman, 2009). To set the notation, assume we have observed ranks at a set of discrete timepoints, indexed by  $t = 0, 1, \dots, T$ . Let  $\boldsymbol{\rho}^{(t)}$  and  $\alpha^{(t)}$  denote the parameters at time  $t$ , and let  $\mathbf{R}_j^{(t)}$ ,  $j = 1, \dots, N_t$  denote the ranks observed at time  $t$ , where  $N_t$  is the number of assessors at time  $t$ . We model the transition between true ranks with the familiar Mallows model,

$$P\left(\boldsymbol{\rho}^{(t)}|\boldsymbol{\rho}^{(t-1)}, \beta\right) = Z_n(\beta)^{-1} \exp\left\{\frac{-\beta}{n}d\left(\boldsymbol{\rho}^{(t)}, \boldsymbol{\rho}^{(t-1)}\right)\right\} 1_{\mathcal{P}_n}\left(\boldsymbol{\rho}^{(t)}\right), \quad (16)$$

for  $t = 1, \dots, T$ , where  $\beta$  describes how strongly the ranks at time  $t$  depend on the ranks at time  $t - 1$ . We assume that the observed ranks at time point  $t$  are conditionally independent of the observed ranks at all other time points, given  $\boldsymbol{\rho}^{(t)}$  and  $\alpha^{(t)}$ , yielding a likelihood contribution

$$P\left(\mathbf{R}_1^{(t)}, \dots, \mathbf{R}_{N_t}^{(t)}|\alpha^{(t)}, \boldsymbol{\rho}^{(t)}\right) = Z_n\left(\alpha^{(t)}\right)^{-1} \exp\left\{\frac{-\alpha^{(t)}}{n}d\left(\mathbf{R}^{(t)}, \boldsymbol{\rho}^{(t)}\right)\right\},$$

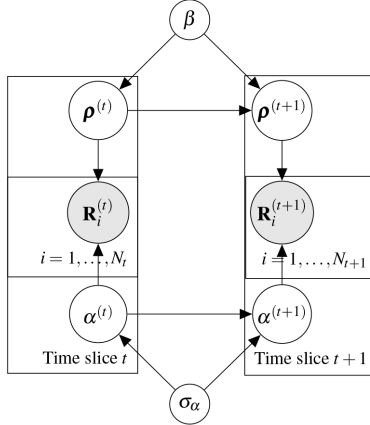


Figure 6: The time dependent rank model represented by a dynamic Bayesian network.

for  $t = 0, \dots, T$ , and a complete data likelihood

$$P(\text{data}|\alpha^{(0:T)}, \boldsymbol{\rho}^{(0:T)}) = \prod_{t=0}^T Z_n(\alpha^{(t)})^{-N_t} \prod_{j=1}^{N_t} \exp\left\{-\frac{\alpha^{(t)}}{n} d(\mathbf{R}_j^{(t)}, \boldsymbol{\rho}^{(t)})\right\}, \quad (17)$$

where we use superscript  $(t_1 : t_2)$  to denote all time points from  $t_1$  up to, and including,  $t_2$ , and *data* denotes all the observed ranks at all time points. Hence, for example  $\alpha^{0:T} = (\alpha^{(0)}, \alpha^{(1)}, \dots, \alpha^{(T)})$ . Finally, we model the transition process of  $\alpha$  simply with the normal distribution, and the constraint  $\alpha^{(t)} \geq 0$ ,

$$P(\alpha^{(t)}|\alpha^{(t-1)}, \sigma_\alpha) = \mathcal{N}(\alpha^{(t-1)}, \sigma_\alpha^2) \times \mathbf{1}_{\mathbb{R}^+}(\alpha^{(t)}), \quad t = 1, \dots, T. \quad (18)$$

For  $\rho^{(0)}$  we use a uniform prior distribution on  $\mathcal{P}_n$ . For  $\alpha^{(0)}$ , we use an exponential prior distribution as before,  $P(\alpha^{(0)}) = \lambda \exp\{-\lambda \alpha^{(0)}\}$ . We use an exponential prior distribution also for  $\beta$ , with the same rate  $\lambda$  as for  $\alpha^{(0)}$ . For  $\sigma_\alpha^2$  we use an inverse gamma distribution,  $P(\sigma_\alpha^2) = IG(a, b)$ , with shape  $a = 1$  and scale  $b = 1$ .

The conditional independence properties assumed in this model are summarized by the dynamic Bayesian network in Figure 6. Our MCMC algorithm alternates between sampling from  $P(\beta|\boldsymbol{\rho}^{(0:T)})$ ,  $P(\boldsymbol{\rho}^{(0:T)}|\text{data}, \alpha^{(0:T)}, \beta)$ ,  $P(\alpha^{(0:T)}|\text{data}, \boldsymbol{\rho}^{(0:T)}, \sigma_\alpha)$ , and  $P(\sigma_\alpha^2|\alpha^{(0:T)})$ . We give full conditional distributions in Appendix A.4.

## 8.1 Student data

We consider a class of students enrolled in a five-year scientific high school program in the Italian town of Lodi. We obtained test results in mathematics for 15 students over their first four years in the school. The number of tests in these years were 5, 4, 8, and 8, respectively. The tests scores were numbers between 0 (worst) and 10 (best), with a precision of one decimal digit. Of the 375 values, a total of 15 were missing, due to students being absent from school on test days. We imputed the missing value using the Gibbs sampler implemented in the R package *mice* (van Buuren and Groothuis-Oudshoorn, 2011), obtaining 20 imputed data sets. Equal numbers of samples were obtained from the posterior distributions using each imputed data set, and the

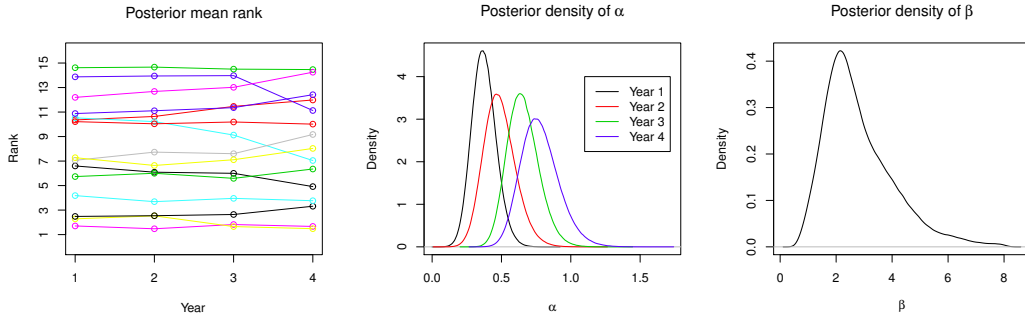


Figure 7: Top: The development of the mean ranks of each student over the four school years analyzed in the example of Section 8.1. Bottom left: Posterior densities of  $\alpha^{(t)}$  for each of the four years. Bottom right: Posterior density of  $\beta$ .

analysis was performed on the joint sample. Within each year, each test was considered an assessor, and the scores were converted to ranks. There were many ties in the data, which were handled by drawing random complete rankings consistent with the data at regular intervals in the MCMC algorithm. We chose to use the Mallows model with the Spearman distance, and an exponential prior distribution with rate  $\lambda = n/20$ .

Figure 7 (left) shows how the mean ranks of the 15 students developed over the four-year period. From this figure one can conclude that the performance of most students remained at a fairly constant level over the first two years, but from the third to the fourth year, there were some students whose rank within the class changed considerably. Figure 7 (center) shows the posterior density of  $\alpha^{(t)}$  in each of the years. It is interesting to note that  $\alpha^{(t)}$  increases with  $t$ . This indicates that the variation in the students' performances was highest in the first year, and the gradually decreased. Figure 7 (right) shows the posterior density of  $\beta$ , from which it is clear that  $\beta$  is considerable larger than  $\alpha^{(t)}$ ,  $t = 0, 1, 2, 3$ .

## 9 Simulation experiments

The results of the potato experiment, where the true ranks were known to us, give some hints about the comparative performances of the Mallows models with footrule, Kendall, and Spearman distances. In order to do a more systematic analysis, we also performed simulation experiments. Define the true ranking  $\rho = (1, \dots, n)$ . The observed (noisy) rankings  $\mathbf{R}_j$ ,  $j = 1, \dots, n$ , were generated by running  $\rho$  through  $N$  independent sequences of moves the leap-and-shift algorithm. We used the values  $L = 1$  and  $L = 5$  for the leap parameter.  $L = 1$  implies that in each move of the algorithm, only neighboring items can be shuffled.  $L = 5$ , on the other hand, means that items which originally are further away from each other also can be interchanged.

We first investigated how the noise level of the data influences the results by varying the number of leap-and-shift moves applied in the rank generation, while fixing  $N = 10$  and  $n = 20$ . In the  $L = 1$  case the number of moves was gradually increased from 5 to 100, and in the  $L = 5$  case from 5 to 35, in steps of size 5. Next, we investigated how the number of assessors influences the results, by keeping the number of leap-and-shift moves fixed at 50 in the  $L = 1$  case and at 10 in the  $L = 5$  case, and the number of items still at  $n = 20$ , but letting  $N$  increase from 5 to 100 in steps of 5.

Two success measures were defined. First, we computed the posterior probability that the

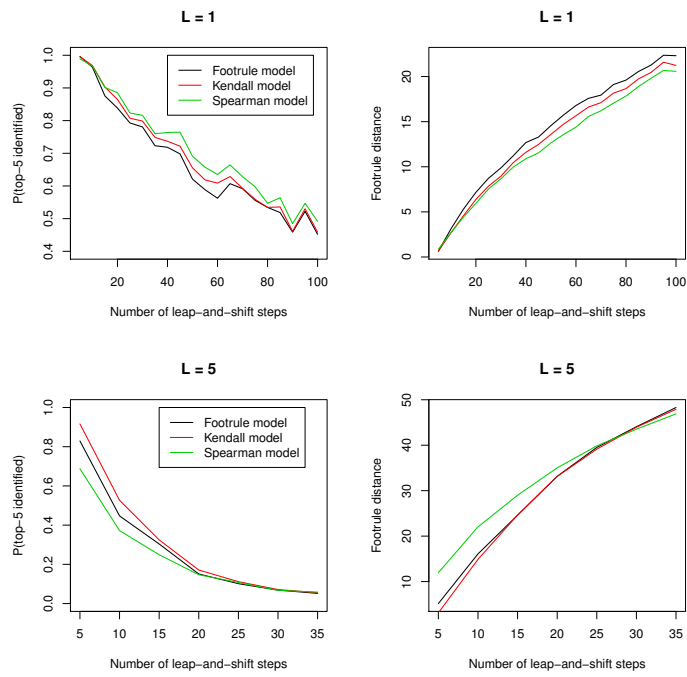


Figure 8: Probability of identifying the top-5 items (left) and the posterior mean footrule distance from the latent ranks to the true ranks (right), as the number of leap-and-shift moves used to generate each observation increases.

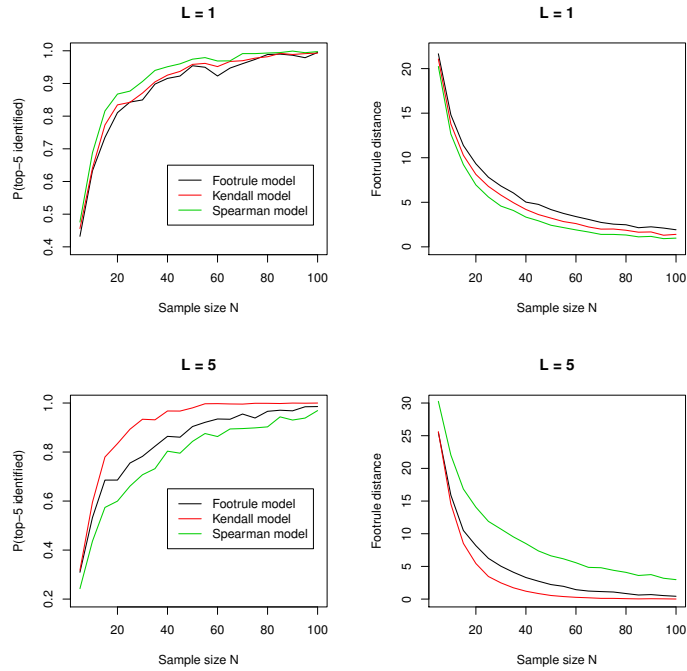


Figure 9: Probability of identifying the top-5 items (left) and posterior mean footrule distance from the latent ranks to the true ranks (right), as  $N$  increases.

true top-5 items were among the five highest ranked items, although not necessarily in the correct order. Next, we computed the posterior mean footrule distance between the latent ranks and the true ranks. In each setting, 200 independent Monte Carlo simulations were run, and we obtained 10000 samples from the posterior distribution for each of these.

Figure 8 shows the results for the setting in which we varied the number of leap-and-shift moves. In the upper row, for which  $L = 1$ , we see a clear ordering: the Mallows model with the Spearman distance performs best, followed by the Kendall distance, and finally the footrule distance. In the bottom row, for which  $L = 5$ , the Spearman model shows the worst performance, both in terms of estimating the top-5 and in terms of minimizing the posterior mean distance to the true ranks. In the  $L = 5$  case, the Kendall model is superior to the others in terms of estimating the top-5, while the Kendall and footrule models show similar performance in terms of minimizing the posterior mean distance to the true ranks.

Next, Figure 9 shows how the results vary with the sample size. The top row shows the case of  $L = 1$ , for which 50 moves of the leap-and-shift algorithm were run to generate each assessor. The bottom row shows the  $L = 5$  case, and here 10 moves of the leap-and-shift algorithm were run. Not surprisingly, we see that the quality of the results increases in the sample size  $N$ . Also, the comparative performances of the different Mallows models are very similar to those seen in Figure 8. When  $L = 1$ , the Spearman distance is the best, followed by the Kendall and footrule distances, while when  $L = 5$ , the Kendall distance is best, followed by the footrule and Spearman distances.

We can interpret the differences between the models used in Figures 8 and 9 by comparing the distance measures. The footrule and Kendall distances are additive in the sense that perturbing

two ranks by one unit off their true value has the same likelihood as perturbing one rank by two units. In other words, if you have already perturbed a rank by one unit, it is as likely to perturb it by yet another unit off as any other, yet unperturbed rank, by one unit from its true position. In the Spearman distance this is no longer the case, because of the square in the exponent. Thus, if occasional bigger displacements come up in the data, as in the  $L = 5$  case, the description given by the Spearman distance is likely to be less fitting. In other words, the inferences provided by the Mallows model with Spearman distance are less robust to larger deviations from true ranks than footrule or Kendall. The Spearman model gives lower posterior probability to latent ranks which are in strong disagreement with some of the assessors, even when the latent rank is in perfect agreement with other assessors.

## 10 Discussion

In this paper, we have developed a fully Bayesian hierarchical framework for the analysis of rank data. An important advantage of the Bayesian approach is that it offers coherently propagated and directly interpretable ways to quantify posterior uncertainties of estimates of any quantity of interest. We extend earlier Bayesian treatments of the Mallows rank model in many respects. We develop an importance sampling scheme for computing the normalizing constant  $Z_n(\alpha)$  based on pseudolikelihood sampling, which allows using the Mallows model with other distance measures than Kendall’s, even when  $n$  is large. Our MCMC algorithm allows efficient sampling from the posterior distribution for the unknown parameters. Motivated by specific data structures, we develop various extensions of the model.

In Section 5 we deal with partial rankings, of which top- $t$  or bottom- $t$  assessments are important cases. In Section 6, we further consider orderings of subsets of items, and particularly the important special case of pairwise comparisons. All of these cases are handled by data augmentation techniques. The method of pairwise comparisons is illustrated for a ranking of 20 football teams in the Premier League. In Section 7 we show how to cluster assessors via mixtures, which is important when there are subpopulations with similar preferences. Performing the clustering within the MCMC algorithm, we allow assessment of posterior uncertainties about the cluster allocation, as well as the scale parameter  $\alpha_c$  and the latent cluster center  $\boldsymbol{\rho}_c$  in each cluster  $c$ . We illustrate the clustering method on a sushi preference dataset with  $n = 10$  items and  $N = 5000$  assessors. In Section 8 we develop a framework for analysis of ranks observed at different time points, which allows us to study how preferences vary in time. We illustrate the method by ranking high school students in each of four consecutive years, using each year’s tests as assessors.

Mallows models may not be computationally feasible when the number of items is very large, e.g.  $n \geq 10^4$ , which is common, e.g., for search engines (ranking of  $n$  documents) and in ranking millions of players in online games (Volkovs and Zemel, 2014). For the Mallows models with the footrule and Spearman distances, there exist asymptotic approximations for  $Z_n(\alpha)$  as  $n$  grows: Mukherjee (2013, Sec. 3.2) shows that an approximation for  $Z_n(\alpha)$  with the Spearman distance works well when  $n = 10^4$ . The main bottleneck appears therefore not to be the computation of  $Z_n(\alpha)$ , but rather the fact that the MCMC algorithm needs to explore the space  $\mathcal{P}_n$  of  $n!$  permutations. Maximum likelihood estimation of the latent ranks  $\boldsymbol{\rho}$  in the Mallows model, known as Kemeny rank aggregation (Kemeny and Snell, 1962), runs into the same problem when  $n$  gets large (Aledo et al., 2013; Ali and Meilă, 2012). On the other hand, the Mallows model performs very well with a large number of assessors  $N$ , as we show in the sushi example of Section 7. For the case of very large  $n$ , Volkovs and Zemel (2014) developed the multinomial preference model (MPM) along the lines of the Bradley-Terry (Bradley and Terry, 1952) and Plackett-Luce

(Luce, 1959; Plackett, 1975) models. The MPM estimates a continuous score for each item, which is converted to the rank scale after the inference algorithm is finished. These scores can be computed by maximizing a concave log-likelihood function, and the MPM thus seems a useful choice when  $n$  is very large and real time performance is needed.

All methods presented in this paper have been implemented in C++ code, which can easily be called from R using the `Rcpp` package (Eddelbuettel and François, 2011; Eddelbuettel, 2013). Neither the code nor the algorithms have been optimized for speed, but still the examples in this paper run efficiently on a standard desktop computer: Obtaining a sufficiently large sample from the posterior distribution in the potato experiment with full data (Section 4) takes a few seconds. Inference for top- $t$  ranking of potatoes (Section 5) and ranking of football teams based on pairwise comparisons (Section 6), takes a few minutes, as these examples involve massive data augmentation in each step of the MCMC algorithm. The software is freely available from the authors, and we are preparing an R package.

## 10.1 Possible extensions of the model

In the framework for modelling time-dependent ranks in Section 8, we assumed that all items were ranked at each time step. However, in reality it may happen that some items which were not available at an early time point  $t$  become available at a later time point  $t + \delta$  (Caron and Teh, 2012), e.g., a new movie or a new type of food. Other items might disappear from the pool, like products which are no longer available on the market. If one is interested in the latent ranks of all items at all times, also at time points when they were not assessed, the data augmentation approach of Section 5 could be used. In this way, for an item not being assessed at time  $t$ , its observed ranks at other time points would contribute to its latent rank at time  $t$  through the transition process (16). If, on the other hand, for a given time point one is only interested in the items which were assessed at that time point, (16) would only take into account the intersection of items present at times  $t$  and  $t - 1$ .

Another interesting problem is how to handle pairwise preferences which are inconsistent with any linear ordering of the items, e.g.,  $\mathcal{A} = \{A_1 \prec A_2, A_2 \prec A_3, A_3 \prec A_1\}$ . One could here create mutually compatible preferences by reversing the order of one or more preferences. This problem is equivalent to creating a DAG by reversing edges in a cyclic graph. Finally, the MCMC algorithm could randomly jump between these consistent preference sets.

The model can also be extended to semi-supervised problems: If the true ranks of a subset of the items were known, we could estimate the reliability of the assessors by the accuracy of their rankings of this subset, and use it as a weight in the Mallows model. Related methods are the Bayesian aggregation of rank data (BARD) by Deng et al. (2014) and the supervised rank aggregation by Liu et al. (2007).

If categorical covariates describing the assessors were available (e.g., age group, gender, nationality), we could develop a hierarchical model of  $G$  groups, with each group  $g$  characterized by a Mallows model with parameters  $\rho_g$  and  $\alpha_g$  which are identically distributed according to common hyperparameters.

Another extension is to incorporate the selection of the number of clusters  $C$  into the probabilistic model, rather than selecting  $C$  based on goodness of fit of  $C$  separate models, each being a mixture of  $1, 2, \dots, C$  Mallows models, respectively. This can be done by exploring the space of models using reversible-jump MCMC (Green, 1995). An alternative would be to use Dirichlet process mixtures, as was done by Meilă and Chen (2010) for generalized Mallows models.

Finally, as the data augmentation step is a potential bottleneck of the MCMC algorithm, significant speedup could be obtained by proposing a new augmented data set, say, at every 100th iteration. It would hence be interesting to study the tradeoff between computational

efficiency and statistical accuracy for the data augmentation problem.

## A Appendix

### A.1 Leap-and-shift distribution

Fix some  $L \in \{1, \dots, n/2\}$  and let  $U \sim \mathcal{U}\{1, \dots, n\}$ . The *leap* step is then described by

$$\begin{aligned} P_L(\boldsymbol{\rho}^* | \boldsymbol{\rho}) &= \sum_{u=1}^n P_L(\boldsymbol{\rho}^* | U = u, \boldsymbol{\rho}) P(U = u) \\ &= \frac{1}{2nL} \sum_{u=1}^n \left\{ 1_{\{L+1, \dots, n-L\}}(\rho_u) \times 1_{\{\rho_u-L, \dots, \rho_u+L\} \setminus \{\rho_u\}}(\rho_u^*) + 1_{\{1, \dots, L\}}(\rho_u) \right. \\ &\quad \times 1_{\{1, \dots, 2L\} \setminus \{\rho_u\}}(\rho_u^*) + 1_{\{n-L+1, \dots, n\}}(\rho_u) \times 1_{\{n-2L+1, \dots, n\} \setminus \{\rho_u\}}(\rho_u^*) \left. \right\} \times 1_{\{\rho_{-u}\}}(\boldsymbol{\rho}_{-u}^*), \end{aligned} \quad (19)$$

where  $\boldsymbol{\rho}_{-u} = (\rho_i \forall i \neq u)$ . Sampling from  $P_L(\boldsymbol{\rho}^* | \boldsymbol{\rho})$  yields  $\boldsymbol{\rho}^* \notin \mathcal{P}_n$ , so there exists a unique pair of integers  $(r, s)$  such that  $\rho_i^* = \rho_j^* = r$  for some  $i \neq j$  and  $s \notin \boldsymbol{\rho}^*$ . Now define the vector  $\boldsymbol{\rho}'$  with elements

$$\rho'_i = \begin{cases} \rho_i^* + 1 & \text{if } s > r \text{ and } i \in [i : \rho_i^* \in \{r, r+1, \dots, s-1\}]; \\ \rho_i^* - 1 & \text{if } s < r \text{ and } i \in [i : \rho_i^* \in \{s+1, s+2, \dots, r\}]; \\ \rho_i^* & \text{otherwise,} \end{cases} \quad (20)$$

for  $i = 1, \dots, n$ , where  $(r, s)$  is the unique pair of integers defined above. The shift operator (20) yields  $\boldsymbol{\rho}' \in \mathcal{P}_n$ . The leap and shift algorithm described here is symmetric, and therefore the  $g(\cdot | \cdot)$  terms in (7) cancel.

### A.2 Importance sampling

Given  $\alpha$ ,  $Z_n(\alpha)$  can be seen as the expectation of  $f_\alpha(\boldsymbol{\rho}) = n! \times \exp((-\alpha/n)d(\boldsymbol{\rho}, \mathbf{P}))$ , for an arbitrary  $\mathbf{P} \in \mathcal{P}_n$ , with  $\boldsymbol{\rho}$  uniformly distributed on  $\mathcal{P}_n$ , i.e.,

$$Z_n(\alpha) = \sum_{\boldsymbol{\rho} \in \mathcal{P}_n} \frac{f_\alpha(\boldsymbol{\rho})}{n!} = \sum_{\boldsymbol{\rho} \in \mathcal{P}_n} f_\alpha(\boldsymbol{\rho}) \frac{(1/n!)}{q(\boldsymbol{\rho})} q(\boldsymbol{\rho}) = \mathbb{E}_q \left\{ \frac{\exp(-\frac{\alpha}{n}d(\boldsymbol{\rho}, \mathbf{P}))}{q(\boldsymbol{\rho})} \right\}, \quad (21)$$

where  $\mathbb{E}_q\{\cdot\}$  denotes expectation with ranks distributed according to the proposal distribution  $q(\cdot)$ . For rank vectors  $\boldsymbol{\rho}^1, \dots, \boldsymbol{\rho}^K$  sampled from  $q(\boldsymbol{\rho})$ , the importance sampling estimate of the normalizing constant is

$$\hat{Z}_n(\alpha) = \frac{1}{K} \sum_{k=1}^K \frac{\exp(-\frac{\alpha}{n}d(\boldsymbol{\rho}^k, \mathbf{P}))}{q(\boldsymbol{\rho}^k)}. \quad (22)$$

This is an unbiased estimator of  $Z_n(\alpha)$ , and its variance is minimized when  $q(\boldsymbol{\rho})$  equals the joint distribution (2) whose normalizing constant we are computing.

As a proposal distribution for the importance sampler, we use a pseudo-likelihood approximation of the target (2), given by the factorization

$$P(\boldsymbol{\rho}' | \boldsymbol{\rho}) = P(\rho'_n | \boldsymbol{\rho}) P(\rho'_{n-1} | \rho'_n, \boldsymbol{\rho}) \dots P(\rho'_2 | \rho'_3, \dots, \rho'_n, \boldsymbol{\rho}) P(\rho'_1 | \rho'_2, \dots, \rho'_n, \boldsymbol{\rho}). \quad (23)$$

The conditionals appearing in (23) are

$$P(\rho'_n | \boldsymbol{\rho}) = \frac{\exp(-\frac{\alpha}{n}d(\rho'_n, \rho_n)) \times 1_{[1, \dots, n]}(\rho'_n)}{\sum_{\tilde{\rho}'_n \in \{1, \dots, n\}} \exp(-\frac{\alpha}{n}d(\tilde{\rho}'_n, \rho_n))}, \quad (24)$$

$$P(\rho'_{n-1}|\rho'_n, \boldsymbol{\rho}) = \frac{\exp\left(-\frac{\alpha}{n}d(\rho'_{n-1}, \rho_{n-1})\right) \times 1_{[\{1, \dots, n\} \setminus \{\rho'_n\}]}(\rho'_{n-1})}{\sum_{\tilde{\rho}'_{n-1} \in \{1, \dots, n\} \setminus \{\rho'_n\}} \exp\left(-\frac{\alpha}{n}d(\tilde{\rho}'_{n-1}, \rho_{n-1})\right)}, \quad (25)$$

$$P(\rho'_2|\rho'_3, \dots, \rho'_n, \boldsymbol{\rho}) = \frac{\exp\left(-\frac{\alpha}{n}d(\rho'_2, \rho_2)\right) \times 1_{[\{1, \dots, n\} \setminus \{\rho'_3, \dots, \rho'_n\}]}(\rho'_2)}{\sum_{\tilde{\rho}'_2 \in \{1, \dots, n\} \setminus \{\rho'_3, \dots, \rho'_n\}} \exp\left(-\frac{\alpha}{n}d(\tilde{\rho}'_2, \rho_2)\right)}, \quad (26)$$

and

$$P(\rho'_1|\rho'_2, \dots, \rho'_n, \boldsymbol{\rho}) = 1_{[\{1, \dots, n\} \setminus \{\rho'_2, \dots, \rho'_n\}]}(\rho'_1). \quad (27)$$

A  $\boldsymbol{\rho}^k$  generated by sampling its  $n$  components sequentially from (24)-(27), has probability  $P(\rho_n^k|\boldsymbol{\rho}^0)P(\rho_{n-1}^k|\rho_n^k, \boldsymbol{\rho}^0), \dots, P(\rho_2^k|\rho_3^k, \dots, \rho_n^k, \boldsymbol{\rho}^0)$ , where we arbitrarily set  $\boldsymbol{\rho}^0 = \{1, \dots, n\}$ . Here we sample the  $n$ th component of  $\boldsymbol{\rho}^k$ , and continue with the  $(n-1)$ st component, all the way to the fixed first component. This is specified by the order of conditioning in the directional pseudo-likelihood, which is of course completely arbitrary. The normalizing constant of the directional pseudo-likelihood is easily computed as the product of the  $n$  denominators specified in (24)-(27).

### A.3 MCMC for clustering the ranks

To obtain samples from the posterior (15) of the Mallows models mixture, we set up a Metropolis-Hastings within Gibbs scheme. This is articulated in two steps:

1. sample  $\boldsymbol{\rho}_1, \dots, \boldsymbol{\rho}_G$  and  $\alpha_1, \dots, \alpha_C$  with a Metropolis-Hastings step;
2. sample  $\tau_1, \dots, \tau_C$  and  $z_1, \dots, z_N$  with Gibbs-sampler steps.

Step (1) is straightforward, since we can rely on the augmented data formulation, and the parameters  $(\boldsymbol{\rho}_c, \alpha_c)_{c=1, \dots, C}$  are conditionally independent given the cluster labels  $z_1, \dots, z_N$ . The update is thus done through a within-cluster Metropolis-Hastings step.

For step (2), we have to give all full conditionals. Since  $\tau_1, \dots, \tau_C$  are conditionally independent from all other variables given the cluster labels  $z_1, \dots, z_N$ , and the Dirichlet prior is conjugate to the multinomial distribution in (13), we have

$$P(\tau_1, \dots, \tau_C | \boldsymbol{\rho}_1, \dots, \boldsymbol{\rho}_C; \alpha_1, \dots, \alpha_C; z_1, \dots, z_N) = P(\tau_1, \dots, \tau_C | z_1, \dots, z_N) \quad (28)$$

$$\propto P(z_1, \dots, z_N | \tau_1, \dots, \tau_C) \cdot P(\tau_1, \dots, \tau_C) \propto \mathcal{D}(z_1, \dots, z_N; \psi + n_1, \dots, \psi + n_C),$$

where  $\mathcal{D}(\cdot)$  indicates the Dirichlet distribution, and  $n_c = \sum_{j=1}^N 1_c(z_j)$ ,  $c = 1, \dots, C$ . The full conditional for cluster labels is detailed below.

More precisely, at the  $q$ -th iteration of MCMC we perform the following steps:

- Gibbs step: we sample  $\tau_1^q, \dots, \tau_C^q$  from a Dirichlet distribution  $\mathcal{D}(\psi + n_1^{q-1}, \dots, \psi + n_C^{q-1})$ , where  $n_c^{q-1} = \sum_{j=1}^N 1_c(z_j^{q-1})$ ,  $c = 1, \dots, C$ .
- Metropolis-Hastings step: we set  $\boldsymbol{\alpha}^{curr} = \boldsymbol{\alpha}^{q-1}$  and scan the clusters in random order. For the  $c$ -th cluster, we check if  $n_c^{q-1}$  is equal to zero. If this is the case, then only the prior distributions enter the M-H ratios. Otherwise, we propose a new rank vector  $\boldsymbol{\rho}'_c$  from the leap-and-shift proposal distribution, and we accept it according to the M-H ratio

$$\min \left\{ 1, \frac{\exp\left(-\frac{\alpha_c^{curr}}{n} \sum_{j: z_j^{q-1}=c} d(\mathbf{R}_j, \boldsymbol{\rho}'_c)\right)}{\exp\left(-\frac{\alpha_c^{curr}}{n} \sum_{j: z_j^{q-1}=c} d(\mathbf{R}_j, \boldsymbol{\rho}_c^{q-1})\right)} \right\}$$

since the normalizing constants simplify and the ranks have a uniform prior. Then, we propose  $\alpha'_c$  in the following way: if  $C > 1$  and  $c \neq 1, C$ , then  $\alpha'_c \sim \mathcal{U}(\alpha_{c-1}^{curr}, \alpha_{c+1}^{curr})$ ; if  $C > 1$  and  $c = 1$  then  $\alpha'_1 \sim \alpha_2^{curr} \cdot \mathcal{B}(5, 2)$ ; if  $C > 1$  and  $c = C$  then  $\alpha'_C \sim \mathcal{U}(\alpha_{C-1}^{curr}, \alpha_C^{curr} + 1)$ . Finally, if  $C = 1$ , then  $\alpha' \sim \mathcal{N}(\alpha^{curr}, \sigma_\alpha^2)$ , where  $\sigma_\alpha = 0.1$ ; in this last case, the further constraint that  $1(\alpha^{curr} > 0)$  is already specified in the exponential prior for  $\alpha$ . Note that with this sampling strategy the constraint on the components of  $\alpha'$  being increasing is satisfied automatically. The proposed value  $\alpha'$  is accepted according to the M-H ratio

$$\min \left\{ 1, \frac{Z_n(\alpha_c^{curr})^{n_c^{q-1}} \cdot \exp\left(-\frac{\alpha'_c}{n} \sum_{j:z_j^{q-1}=c} d(\mathbf{R}_j, \boldsymbol{\rho}_c^q)\right) \cdot \exp(-\lambda \cdot \alpha'_c)}{Z_n(\alpha'_c)^{n_c^{q-1}} \cdot \exp\left(-\frac{\alpha_c^{curr}}{n} \sum_{j:z_j^{q-1}=c} d(\mathbf{R}_j, \boldsymbol{\rho}_c^q)\right) \cdot \exp(-\lambda \cdot \alpha_c^{curr})} \right\},$$

and if accepted, then  $\alpha_c^{curr} = \alpha'_c$ . When all clusters have been scanned, we set  $\alpha^q = \alpha^{curr}$ .

- Gibbs step: for  $j = 1, \dots, N$ , we sample independently the cluster labels  $z_j^q$  from the distribution

$$P(z_j^q = c | \tau_c^q, \boldsymbol{\rho}_c^q, \alpha_c^q, R_j) \propto \tau_c^q \cdot P(\mathbf{R}_j | \boldsymbol{\rho}_c^q, \alpha_c^q) = \tau_c^q \cdot Z_n(\alpha_c^q)^{-1} \cdot \exp\left(-\frac{\alpha_c^q}{n} d(\mathbf{R}_j, \boldsymbol{\rho}_c^q)\right).$$

#### A.4 Modeling of time-dependent ranks

The conditional distributions required in our MCMC algorithm for time-dependent ranks are

$$\begin{aligned} & P(\boldsymbol{\rho}^{(0:T)} | \text{data}, \alpha^{(0:T)}, \beta) \\ & \propto \left\{ \prod_{t=0}^T P(\mathbf{R}_1^{(t)}, \dots, \mathbf{R}_{N_t}^{(t)} | \alpha^{(t)}, \boldsymbol{\rho}^{(t)}) \right\} \times \left\{ P(\boldsymbol{\rho}^{(0)}) \prod_{t=1}^T P(\boldsymbol{\rho}^{(t)} | \boldsymbol{\rho}^{(t-1)}, \beta) \right\} \\ & \propto \exp \left\{ -\sum_{t=0}^T \frac{\alpha^{(t)}}{n} \sum_{j=1}^{N_t} d(\mathbf{R}_j^{(t)}, \boldsymbol{\rho}^{(t)}) - \frac{\beta}{n} \sum_{t=1}^T d(\boldsymbol{\rho}^{(t)}, \boldsymbol{\rho}^{(t-1)}) \right\} \times \left\{ \prod_{t=0}^T 1_{\mathcal{P}_n}(\boldsymbol{\rho}^{(t)}) \right\}, \\ & P(\alpha^{(0:T)} | \text{data}, \boldsymbol{\rho}^{(0:T)}, \sigma_\alpha) \\ & \propto \left\{ \prod_{t=0}^T P(\mathbf{R}_1^{(t)}, \dots, \mathbf{R}_{N_t}^{(t)} | \alpha^{(t)}, \boldsymbol{\rho}^{(t)}) \right\} \times \left\{ P(\alpha^{(0)}) \prod_{t=1}^T P(\alpha^{(t)} | \alpha^{(t-1)}, \sigma_\alpha^2) \right\} \\ & \propto \left\{ \prod_{t=0}^T Z_n(\alpha^{(t)})^{-N_t} \right\} \times \\ & \quad \exp \left\{ -\sum_{t=0}^T \frac{\alpha^{(t)}}{n} \sum_{j=1}^{N_t} d(\mathbf{R}_j^{(t)}, \boldsymbol{\rho}^{(t)}) - \sum_{t=1}^T \frac{(\alpha^{(t)} - \alpha^{(t-1)})^2}{2\sigma_\alpha^2} - \lambda \alpha^{(0)} \right\}, \\ & P(\beta | \boldsymbol{\rho}^{(0:T)}) \propto \left\{ \prod_{t=1}^T Z_n(\beta)^{-1} \right\} \times \exp \left\{ \frac{-\beta}{n} \sum_{t=1}^T d(\boldsymbol{\rho}^{(t)}, \boldsymbol{\rho}^{(t-1)}) - \lambda \beta \right\}, \end{aligned}$$

and

$$P(\sigma_\alpha^2 | \alpha^{(0:T)}) \propto P(\sigma_\alpha^2) \times \prod_{t=1}^T P(\alpha^{(t)} | \alpha^{(t-1)}, \sigma_\alpha^2)$$

$$\propto (\sigma_\alpha^2)^{-(a+T/2)-1} \exp \left\{ - \left( b + \frac{1}{2} \sum_{t=1}^T (\alpha^{(t)} - \alpha^{(t-1)})^2 \right) \frac{1}{\sigma_\alpha^2} \right\}.$$

$P(\sigma_\alpha^2 | \alpha^{(0:T)})$  is an inverse gamma distribution with shape  $a + T/2$  and scale

$$b + \frac{1}{2} \sum_{t=1}^T (\alpha^{(t)} - \alpha^{(t-1)})^2,$$

which means that we have a nice conjugacy property for  $\sigma_\alpha^2$ . In order to sample from the first three conditionals, we need to use the Metropolis-Hastings algorithm.

## References

- Afsari, B., U. B. Neto, and D. Geman (2014). Rank discriminants for predicting phenotypes from RNA expression. *Annals of Applied Statistics*, to appear.
- Aledo, J. A., J. A. Gàmez, and D. Molina (2013). Tackling the rank aggregation problem with evolutionary algorithms. *Applied Mathematics and Computation* 222, 632 – 644.
- Ali, A. and M. Meilă (2012). Experiments with Kemeny ranking: What works when? *Mathematical Social Sciences* 64(1), 28 – 40. Computational Foundations of Social Choice.
- Baker, R. D. and I. G. McHale (2014). Time varying ratings in association football: the all-time greatest team is... *J. R. Statist. Soc. A*, to appear.
- Bradley, R. A. and M. E. Terry (1952). Rank analysis of incomplete block designs: I. the method of paired comparisons. *Biometrika* 39(3), 324–345.
- Busse, L. M., P. Orbanz, and J. M. Buhmann (2007). Cluster analysis of heterogeneous rank data. In *Proceedings of the 24th International Conference on Machine Learning, ICML '07*, New York, NY, USA, pp. 113–120. ACM.
- Caron, F. and Y. W. Teh (2012). Bayesian nonparametric models for ranked data. In F. Pereira, C. Burges, L. Bottou, and K. Weinberger (Eds.), *Advances in Neural Information Processing Systems 25*, pp. 1520–1528. Curran Associates, Inc.
- Caron, F., Y. W. Teh, and T. B. Murphy (2014). Bayesian nonparametric Plackett-Luce models for the analysis of preferences for college degree programmes. *Annals of Applied Statistics*, to appear.
- Celeux, G., M. Hurn, and C. P. Robert (2000). Computational and inferential difficulties with mixture posterior distributions. *J. Am. Statist. Ass.* 95(451), pp. 957–970.
- Deng, K., S. Han, K. J. Li, and J. S. Liu (2014). Bayesian aggregation of order-based rank data. *J. Am. Statist. Ass.*, to appear.
- Diaconis, P. (1988). *Group representations in probability and statistics*. Lecture Notes - Monograph series 11. Hayward, CA: Institute of Mathematical Statistics.
- Diaconis, P. and R. L. Graham (1977). Spearman’s footrule as a measure of disarray. *J. R. Statist. Soc. B* 39(2), 262–268.

- Eddelbuettel, D. (2013). *Seamless R and C++ Integration with Rcpp*, Volume 64 of *Use R!* New York, NY: Springer.
- Eddelbuettel, D. and R. François (2011). Rcpp: Seamless R and C++ integration. *Journal of Statistical Software* 40(8), 1–18.
- Falmagne, J.-C. (1996). A stochastic theory for the emergence and the evolution of preference relations. *Mathematical Social Sciences* 31(2), 63 – 84.
- Fligner, M. A. and J. S. Verducci (1986). Distance based ranking models. *J. R. Statist. Soc. B* 48(3), 359–369.
- Fligner, M. A. and J. S. Verducci (1990). Posterior probabilities for a consensus ordering. *Psychometrika* 55(2), 53–63.
- Green, P. J. (1995). Reversible jump Markov chain Monte Carlo computation and Bayesian model determination. *Biometrika* 82(4), 711–732.
- Jasra, A., C. C. Holmes, and D. A. Stephens (2005). Markov chain Monte Carlo methods and the label switching problem in Bayesian mixture modeling. *Statistical Science* 20(1), 50–67.
- Kamishima, T. (2003). Nantonac collaborative filtering: Recommendation based on order responses. In *Proceedings of the Ninth ACM SIGKDD International Conference on Knowledge Discovery and Data Mining, KDD '03*, New York, NY, USA, pp. 583–588. ACM.
- Kemeny, J. G. and J. L. Snell (1962). *Mathematical Models in the Social Sciences*. New York, NY: Blaisdell.
- Koller, D. and N. Friedman (2009). *Probabilistic Graphical Models*. Adaptive computation and machine learning series. Cambridge, MA: MIT Press.
- Liu, Y.-T., T.-Y. Liu, T. Qin, Z.-M. Ma, and H. Li (2007). Supervised rank aggregation. In *Proceedings of the 16th International Conference on World Wide Web, WWW '07*, New York, NY, USA, pp. 481–490. ACM.
- Lu, T. and C. Boutilier (2011, June). Learning Mallows models with pairwise preferences. In L. Getoor and T. Scheffer (Eds.), *Proceedings of the 28th International Conference on Machine Learning (ICML-11)*, ICML '11, New York, NY, USA, pp. 145–152. ACM.
- Luce, R. D. (1959). *Individual choice behavior: A theoretical analysis*. New York, NY: Wiley.
- Mallows, C. L. (1957). Non-null ranking models. *Biometrika* 44(1-2), 114–130.
- Marden, J. I. (1995). *Analyzing and Modeling rank Data*, Volume 64 of *Monographs on Statistics and Applied Probability*. Cambridge, MA: Chapman & Hall.
- Margolin, A. A., I. Nemenman, K. Basso, C. Wiggins, G. Stolovitzky, R. D. Favera, and A. Califano (2006). ARACNE: An algorithm for the reconstruction of gene regulatory networks in a mammalian cellular context. *BMC Bioinformatics* 7(Suppl 1), S7.
- Meilă, M. and H. Chen (2010). Dirichlet process mixtures of generalized Mallows models. In P. Grünwald and P. Spirtes (Eds.), *Proceedings of the Twenty-Sixth Conference on Uncertainty in Artificial Intelligence (UAI2010)*. AUAI Press.
- Meyer, D. and K. Hornik (2009). Generalized and customizable sets in R. *Journal of Statistical Software* 31(2), 1–27.

- Meyer, D. and K. Hornik (2014). *relations: Data Structures and Algorithms for Relations*. R package version 0.6-3.
- Mukherjee, S. (2013). Estimation of parameters in non uniform models on permutations. *ArXiv e-prints*.
- Murphy, T. B. and D. Martin (2003). Mixtures of distance-based models for ranking data. *Computational Statistics & Data Analysis* 41(3-4), 645–655.
- Plackett, R. L. (1975). The analysis of permutations. *Appl. Statist.* 24(2), 193–202.
- Regenwetter, M., J.-C. Falmagne, and B. Grofman (1999). A stochastic model of preference change and its application to 1992 presidential election panel data. *Psychological Review* 106(2), 362–384.
- Stephens, M. (2000). Dealing with label switching in mixture models. *J. R. Statist. Soc. B* 62(4), 795–809.
- Tanner, M. A. and W. H. Wong (1987). The calculation of posterior distributions by data augmentation. *J. Am. Statist. Ass.* 82(398), pp. 528–540.
- van Buuren, S. and K. Groothuis-Oudshoorn (2011). mice: Multivariate imputation by chained equations in R. *Journal of Statistical Software* 45(3), 1–67.
- Volkovs, M. N. and R. S. Zemel (2014). New learning methods for supervised and unsupervised preference aggregation. *Journal of Machine Learning Research* 15, 1135–1176.

## Supplementary material

### B Potato experiment

#### B.1 Data collection

Figure S10 shows the 20 potatoes laid out on a plate, marked by letters from A to T. Figure S11 shows some of the assessors performing the visual inspection part of the experiment. Table S3 shows the ranks given by the 12 assessors in the visual inspection experiment, and Table S4 shows the ranks given in the weighing experiment.

#### B.2 Posterior distributions for ranks

Figure S12 shows the cumulative distribution functions for the total distance between the latent ranks and the true ranks, as measured by the Kendall and Spearman distance, similar to Figure 2 in the main paper, which uses the footrule distance. We see that the Mallows model with the footrule and Kendall distances are best in the weighing experiment, while the Mallows model with the Spearman distance is best in the visual inspection experiment.

Figures S13 and S14 show a selection of results from the two potato experiments. In both experiments, the estimated rank of the heaviest and lightest potatoes have strongly peaked distributions, while the distributions of the median potatoes have a larger spread. The improved precision of the weighing experiment over the visual one is also evident from comparing these two figures.



Figure S10: The 20 potatoes labeled by letters A-T.



Figure S11: The photo shows some of the assessors performing the visual inspection part of the experiment.

Table S3: Ranks given by the 12 assessors (rows) to the 20 potatoes (columns) in the visual inspection experiment. The true ranks, and the true weights in grams, are given in the two bottom rows.

	A	B	C	D	E	F	G	H	I	J	K	L	M	N	O	P	Q	R	S	T
1	10	18	19	15	6	16	4	20	3	5	12	1	2	9	17	8	7	14	13	11
2	10	18	19	17	11	15	6	20	4	3	13	1	2	7	16	8	5	12	9	14
3	12	15	18	16	13	11	7	20	6	3	8	2	1	4	19	5	9	14	10	17
4	9	17	19	16	10	15	5	20	3	4	8	1	2	7	18	11	6	13	14	12
5	12	17	19	15	7	16	2	20	3	9	13	1	4	5	18	11	6	8	10	14
6	10	15	19	16	8	18	6	20	3	7	11	1	2	4	17	9	5	13	12	14
7	9	16	19	17	10	15	5	20	3	8	11	1	2	6	18	7	4	14	12	13
8	14	18	20	19	11	15	6	17	4	3	10	1	2	7	16	8	5	12	9	13
9	8	16	18	19	12	13	6	20	5	3	7	1	4	2	17	10	9	15	14	11
10	7	17	19	18	9	15	5	20	3	10	11	1	2	6	16	8	4	13	12	14
11	12	16	19	15	13	18	7	20	3	5	11	1	2	6	17	10	4	14	8	9
12	14	15	19	16	12	18	8	20	3	4	9	1	2	7	17	6	5	13	10	11
True rank	11	17	19	16	10	15	5	20	3	4	9	1	2	6	18	7	8	14	12	13
True weight	73	56	50	59	77	62	87	46	95	89	78	115	99	86	54	85	80	68	72	71

Table S4: Ranks given by the 12 assessors (rows) to the 20 potatoes (columns) in the weighing experiment. The true ranks, and the true weights in grams, are given in the two bottom rows.

	A	B	C	D	E	F	G	H	I	J	K	L	M	N	O	P	Q	R	S	T
1	10	17	19	15	6	16	4	20	2	5	11	1	3	7	18	8	9	14	12	13
2	13	18	19	16	10	15	5	20	4	3	12	1	2	6	17	8	7	11	9	14
3	11	16	20	15	10	14	6	19	9	4	7	1	3	2	18	5	8	17	12	13
4	10	17	19	16	11	15	5	20	3	4	9	1	2	6	18	8	7	12	14	13
5	11	17	19	16	6	15	4	20	2	8	12	1	3	5	18	10	7	13	9	14
6	9	16	18	15	10	17	8	19	3	7	11	2	1	4	20	5	6	14	12	13
7	9	17	19	16	11	15	5	20	3	8	10	1	2	7	18	6	4	14	12	13
8	12	17	19	18	9	15	5	20	3	4	10	1	2	8	16	7	6	14	11	13
9	9	16	19	18	12	14	6	20	5	2	8	1	4	3	17	10	7	15	13	11
10	10	17	19	16	7	15	4	20	3	9	11	1	2	5	18	8	6	13	12	14
11	11	16	18	15	12	17	7	20	3	4	10	1	2	6	19	8	5	14	9	13
12	12	16	19	15	10	17	8	20	3	4	9	1	2	6	18	5	7	14	11	13
True rank	11	17	19	16	10	15	5	20	3	4	9	1	2	6	18	7	8	14	12	13
True weight	73	56	50	59	77	62	87	46	95	89	78	115	99	86	54	85	80	68	72	71

Table S5: The posterior probability of being among the top-5 for each potato in the visual inspection experiment. Boldface numbers show significant findings at the 95 % level, while asterisks indicate potatoes which are wrongly assessed to be top-5.

Visual		$P(\text{top-5})$			
Rank	Potato	Footrule	Kendall	Spearman	Mean
1	L	<b>1.00</b>	<b>1.00</b>	<b>1.00</b>	1.08
2	M	<b>1.00</b>	<b>1.00</b>	<b>1.00</b>	2.25
3	I	<b>1.00</b>	<b>1.00</b>	<b>1.00</b>	3.58
4	J	<b>0.997</b>	<b>0.961</b>	0.882	5.33
5	G	0.107	0.173	0.603	5.58
6	N	0.006	0.013	0.206	5.83
7	P	0.000	0.000	0.000	8.42
8	Q	0.890*	0.852*	0.310	5.75
9	K	0.000	0.000	0.000	10.33
	⋮	⋮	⋮	⋮	⋮
20	H	0.000	0.000	0.000	19.75

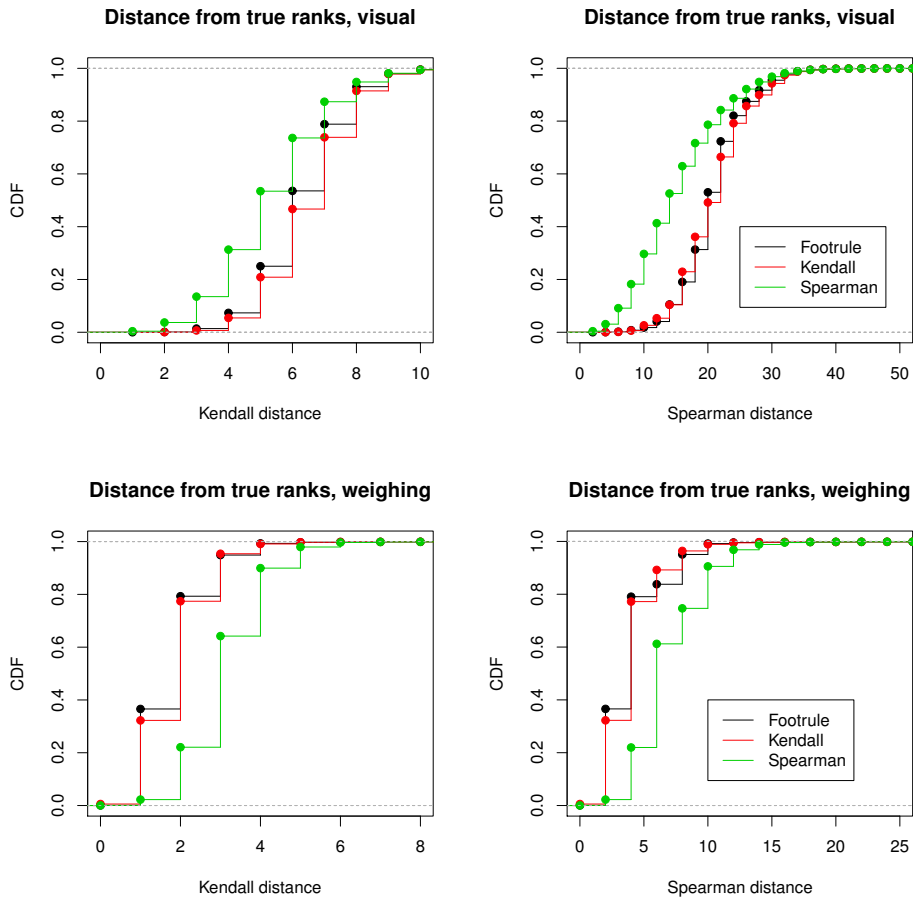


Figure S12: The posterior distributions, expressed in terms of the CDFs for the total distance between the latent and true ranks when measured by the Kendall distance (left), and Spearman distance (right). The blue curves represent the posterior distributions for the latent ranks in the Mallows model with the footrule distance, the red curves with the Kendall distance, and the green curves with the Spearman distance.

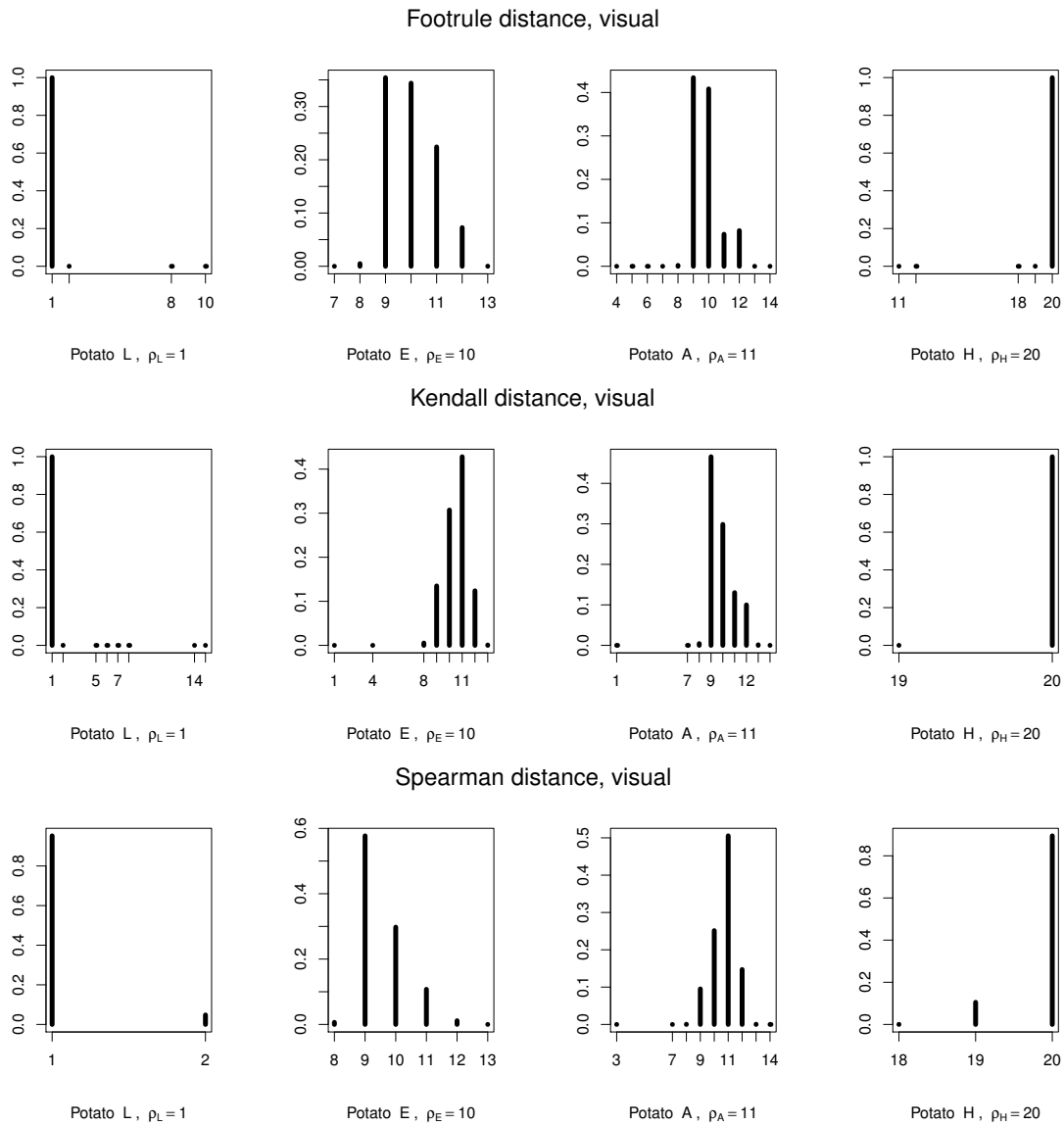


Figure S13: Ranks estimated from the Mallows models in the visual inspection experiment, for the potatoes with true ranks 1 (heaviest), 10, 11 (middle), and 20 (lightest).

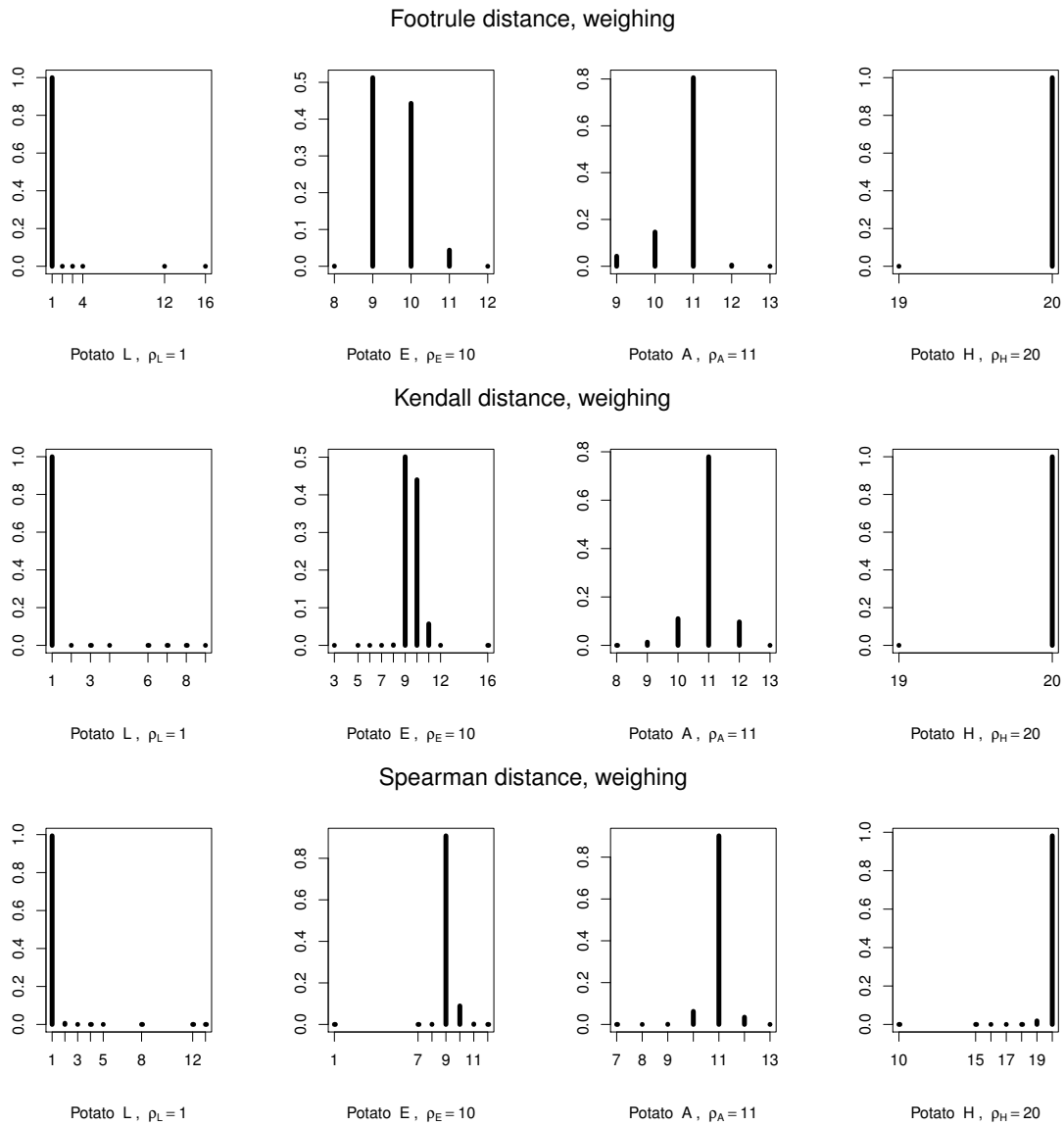


Figure S14: Ranks estimated from the Mallows models in the weighing experiment, for the potatoes with true ranks 1 (heaviest), 10, 11 (middle), and 20 (lightest).

Table S6: The posterior probability of being among the top-5 for each potato in the visual inspection experiment. Boldface numbers show significant findings at the 95 % level, while asterisks indicate potatoes which are wrongly assessed to be top-5.

Weighing		$P(\text{top-5})$			
Rank	Potato	Footrule	Kendall	Spearman	Mean
1	L	<b>1.00</b>	<b>1.00</b>	<b>1.00</b>	1.08
2	M	<b>1.00</b>	<b>0.999</b>	<b>1.00</b>	2.33
3	I	<b>1.00</b>	<b>1.00</b>	<b>1.00</b>	3.58
4	J	<b>1.00</b>	<b>0.997</b>	<b>0.960</b>	5.17
5	G	0.936	0.866	0.315	5.58
6	N	0.065	0.138	0.725*	5.42
7	P	0.000	0.000	0.000	7.33
	⋮	⋮	⋮	⋮	⋮
20	H	0.000	0.000	0.000	19.83

The Bayesian approach easily allows us to explore the uncertainty about the estimated ranks. We consider the case of identifying the set of top-5 potatoes, neglecting their order. For each of the three models, the posterior probability of being among the top-5 was computed for each potato. Tables S5 shows the results for the visual inspection experiment. The potatoes are listed according to their true rank, and the mean ranking provided by the assessors is presented in the rightmost column. Columns 3, 4, and 5 show, for each potato, the posterior probability that it is among the top-5. Defining the estimated top-5 set as the five potatoes with highest posterior probability, numbers in boldface indicate that the potato is significantly assessed to be top-5 at a 95% confidence level, while an asterisk indicates that the potato was erroneously included in the top-5 set. In Table S5, we see that the Spearman model is the only one which identifies the correct set of potatoes in the visual inspection experiment, although only three of these are significant. Both the footrule and the Kendall model give potato Q, whose true rank is 8, a high probability of being among the top-5. The high posterior ranking given to potato Q can also be seen in the top left and center heat plots in Figure 1 of the main paper, as the red/yellow square which stands out below the diagonal at position 8 on the horizontal axis.

Table S6 shows the corresponding numbers from the weighing experiment. Here, both the footrule and Kendall model correctly identify the top-5, while the Spearman model includes potato N (true rank 6) instead of potato G (true rank 5).

To summarize, Tables S5 and S6 as well as Figures S13 and S14 illustrate how the Bayesian framework easily allows us to quantify our uncertainty about any estimates. In addition, our methods allow for comparison of the posterior distributions obtained from the Mallows models with different distance measures, in contrast to most earlier work which have only used the Kendall distance. Here, it is clear that the footrule distance performs best in the weighing experiment, while the Spearman distance performs in the visual experiment.

### B.3 Top-5 estimation in the visual inspection part of the potato experiment

In Section 5.1 of the main paper, we show the results of estimating the five heaviest potatoes based on either the top-5 or the top-10 rankings provided by each assessor in the weighing experiment. In Figure S15 we show the corresponding results for the visual inspection experiment. It is

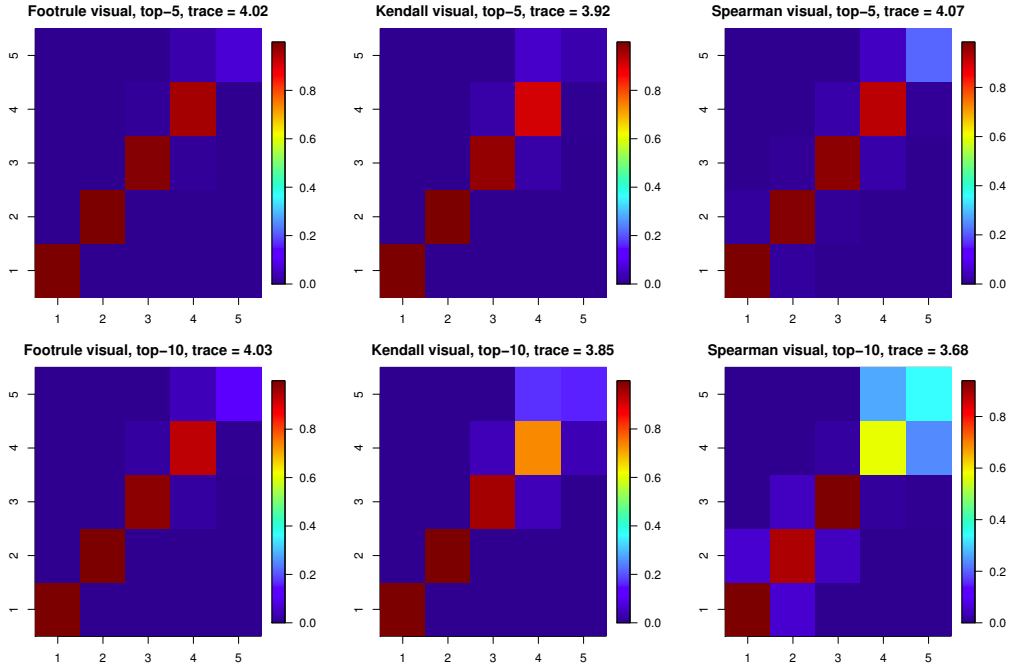


Figure S15: Estimation of the five heaviest potatoes when using only the five highest ranks from each assessor (top), and when using only the ten highest ranks from each assessor (bottom).

clear that the Mallows model with the footrule distance performs better than with the Kendall distance. For these two distances, the results are almost identical when using top-5 or top-10 data, while the model with the Spearman distance performs considerably better when using the top-5 data, as compared to the top-10 data.

## B.4 Impact of prior distribution in potato experiment

Here we describe experiments conducted in order to test the impact of the prior distribution for  $\alpha$  on the results in our analyses.

### B.4.1 Full data

In the potato experiment with full data, described in Section 4 of the main paper, we used an exponential prior for  $\alpha$  with rate  $\lambda = 1/10$ . Here we investigate the impact of this prior distribution for the Mallows model with the *footrule* distance in the *visual* experiment. The same type of analysis for the other Mallows models, as well as in the *weighing* experiment, gave similar results. An exponential distribution with rate  $\lambda$  has mean  $1/\lambda$ , and variance  $1/\lambda^2$ , so a large value of  $\lambda$  implies a strong *a priori* assumption that  $\alpha$  is close to zero, and a correspondingly low precision in the measurements made by the assessors.

Figure S16 shows how the prior distribution of  $\alpha$  influences the result. "Uniform" denotes a uniform improper prior distribution on the positive half line,  $\pi(\alpha) = \mathcal{U}(0, \infty)$ . We see that the uniform prior and the exponential prior with  $\lambda = 1/10$  gave nearly identical posterior distributions of  $\alpha$ , as well as posterior distribution of the distance from the estimated ranks to the true ranks. Setting  $\lambda = 1$  resulted in a shift in the posterior distribution of  $\alpha$ , but the distance to

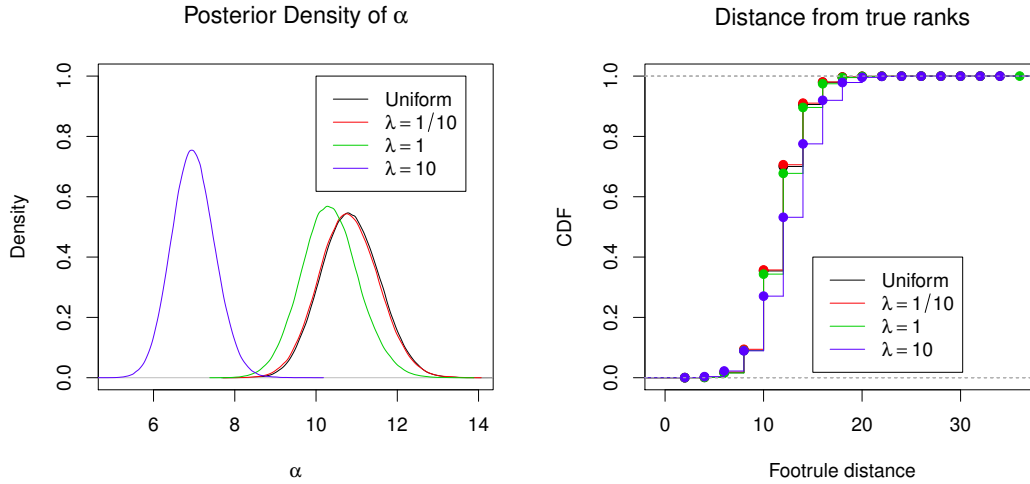


Figure S16: Impact of the prior distribution in the potato experiment with full data, described in Section 4 of the main paper. Results are shown for the Mallows model with the footrule distance in the visual inspection experiment.

the true ranks was nearly unchanged. On the other hand, setting  $\lambda = 10$  gave a strong shift to the left of the posterior distribution of  $\alpha$ , and a clearly larger distance from the estimated ranks to the true ranks. We conclude that the model seems robust to small variations in the choice of  $\lambda$  in this case. Both  $\lambda = 1$  and  $\lambda = 10$  imply a very strong prior assumption that  $\alpha$  is close to zero, and the model still produced reasonable results in these situations, with quite modest sample size.

#### B.4.2 Top-5 rankings

In the top-5 experiment described in Section 5.1, we used less data than in the full data experiment. One could therefore suspect that the prior distribution is more important in this case. We repeated the experiment described in Section B.4.2 above, by testing  $\pi(\alpha) = \mathcal{U}(0, \infty)$ , as well as the exponential distribution with rate  $\lambda \in \{1/10, 1, 10\}$ .

Figure S17 shows the resulting heat plots for the four different prior distributions, for the Mallows model with the footrule distance, using the top-5 rankings of each assessors in the visual inspection experiment. Again we see that the results were essentially equal for the uniform prior as well as  $\lambda = 1/10$  and  $\lambda = 1$ . The extreme value  $\lambda = 10$ , on the other hand, yielded considerably worse performance.

## C Ranking of football teams

The data used in this example can be downloaded from [http://www.clearlyandsimply.com/files/2010/05/premier\\_league.zip](http://www.clearlyandsimply.com/files/2010/05/premier_league.zip).

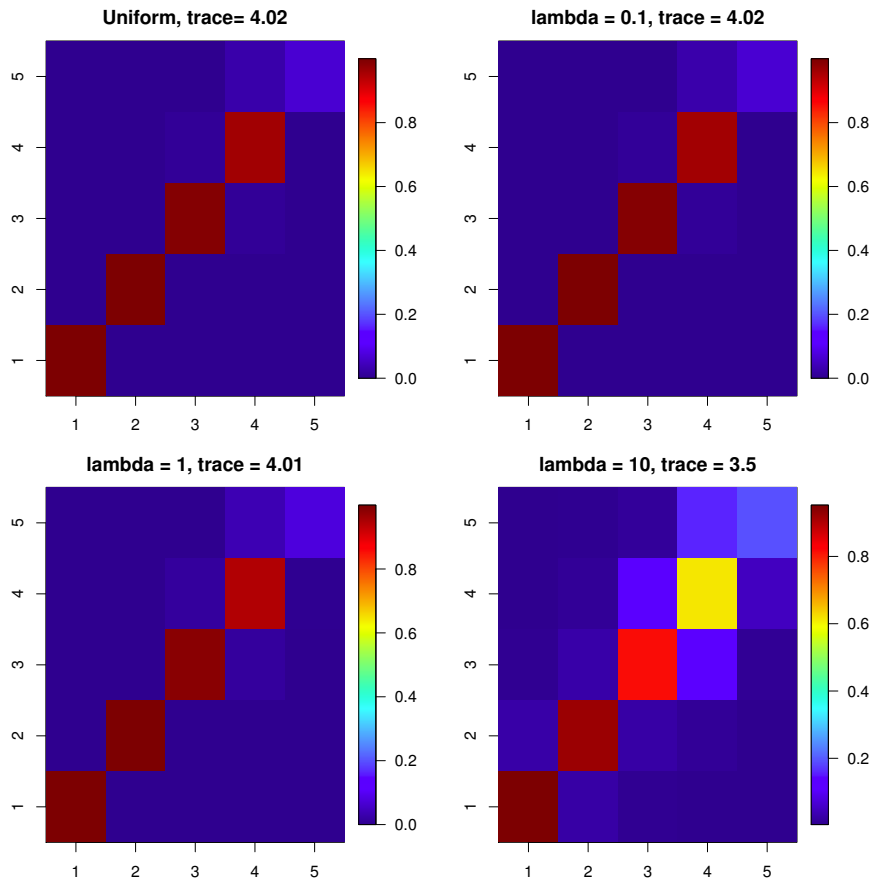


Figure S17: Impact of the prior distribution of  $\alpha$  in the potato experiment, when the top-5 rankings of each assessor in the visual inspection part of the potato experiment were used, for the Mallows model with the footrule distance.

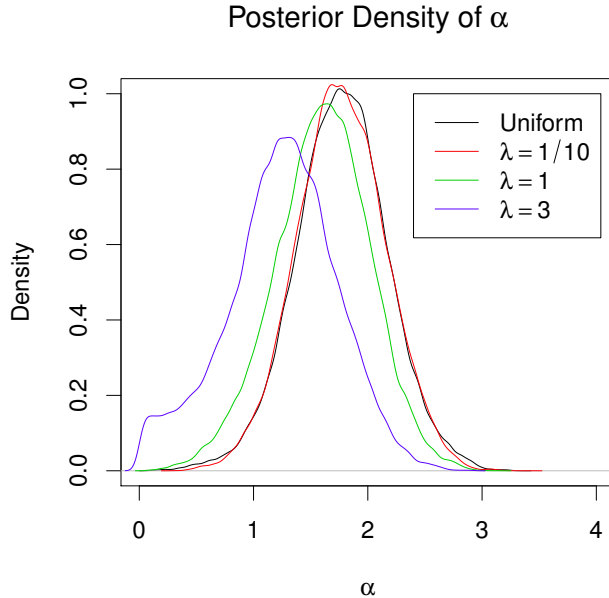


Figure S18: Impact of the prior distribution of  $\alpha$  on its posterior distribution in the ranking of football teams in the Premier League.

### C.1 Impact of prior distribution

We tested the impact of the prior distribution  $\pi(\alpha)$  in the ranking of football teams described in Section 6.1. Figure S18 shows the posterior distribution of  $\alpha$  when using  $\pi(\alpha) = \mathcal{U}(0, \infty)$ , as well as the exponential distribution with rate  $\lambda \in \{1/10, 1, 3\}$ . As before, we observe that the exponential prior with  $\lambda = 1/10$  and the uniform prior on the positive half line gave very similar posterior distributions of  $\alpha$ , while  $\lambda = 1$  and  $\lambda = 3$  pulled the posterior distribution towards zero. When setting  $\lambda = 10$  in this case, the values of  $\alpha$  were drawn very close to zero, resulting in a nearly uniform posterior distribution of ranks.

### C.2 Stochastic orderings

The Bayesian approach allows us to easily compute a stochastic ordering of the football teams in the Premier League, corresponding to Figure 4 in the main paper. We used the convention that team  $A_i$  dominates  $A_j$  if

$$P(\rho_i \leq r | \text{data}) \geq P(\rho_j \leq r | \text{data}) \quad \forall r \in \{1, \dots, n\}.$$

Next, we can also compute the posterior probability that team  $A_i$  has a lower rank than  $A_j$ , given by  $P(\rho_i < \rho_j | \text{data})$ . Table S7 summarizes these two measures for all the teams. The number in matrix entry  $(i, j)$  shows  $P(\rho_i < \rho_j | \text{data})$ , and if the number is marked with an asterisk, team  $A_i$  stochastically dominated  $A_j$ . Out of the 190 pairs of teams, 182 were stochastically ordered. The remaining 8 pairs had matrix elements very close to 0.5. For example, the probability that Bolton has a higher rank than Newcastle is 0.51, and these teams are not stochastically ordered.



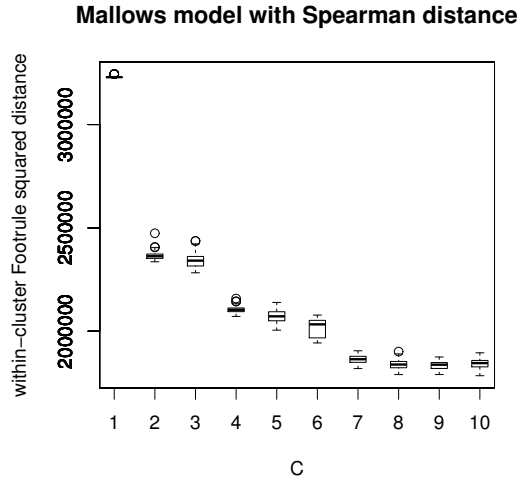


Figure S19: Cluster analysis of the sushi dataset when applying Mallows mixture models with the Spearman distance: boxplots of the posterior distributions of the within-cluster SSE's for different choices of  $C$ .

## D Analysis of sushi data

This dataset consists of sushi preferences surveyed across Japan. These preference data can be freely downloaded from <http://www.kamishima.net/sushi/>.

### D.1 Mixture of Mallows models with Spearman distance

We here report the results obtained with the mixture of Mallows models with Spearman distance, for various choices of  $C$ .

In Figure S19 the boxplot of the posterior distributions of the within-cluster SSE's of sushi data when using a Mallows mixture with Spearman distance are shown with respect to  $C$ . An elbow corresponding to  $C = 7$  is clearly visible in the plot, thus suggesting this number of clusters as the best choice when the Spearman distance is used. Table S8 reports, for  $C = 7$ , the MAP estimates for  $\tau$  and  $\alpha$ , together with their 95% highest posterior density intervals, and the sushi items arranged according to the MAP estimates of cluster centers, for each cluster. There seems to be quite a good agreement between the clustering results obtained here by applying the mixture model with the Spearman distance, and those established when applying the footrule distance, described in the main paper. Five of the six clusters in Table 2 seem to have a close neighbor among the seven clusters listed in Table S8, viz., clusters 1, 2, 3, 4, and 5 in Table 2 have, in this order, clusters 3, 2, 1, 6 and 4 in Table S8 as their neighbors. In addition, cluster 6 in Table 2 appears to combine elements form three clusters in Table S8, viz. numbers 2, 3 and 7. Finally, cluster 5 in Table S8 has no close neighbors amongst those listed in Table 2, the closest one there being number 4. These considerations are confirmed by Figure S23, showing pairwise Spearman distances between the MAP estimates of the cluster centers when applying the Mallows mixture model with the footrule distance and  $C = 6$  (along rows), and the Mallows mixture model with the Spearman distance and  $C = 7$  (along columns).

CDF for the Mallows model with Footrule distar CDF for the Mallows model with Spearman dista

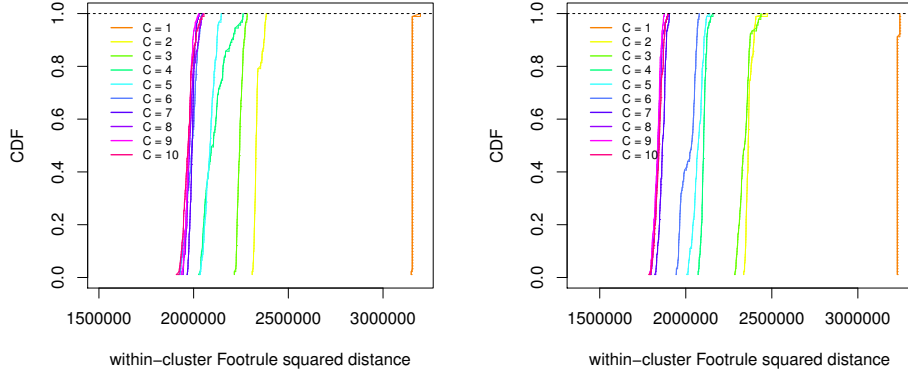


Figure S20: Cluster analysis of the sushi dataset when applying Mallows mixture models with the footrule (left) and Spearman (right) distance: posterior cumulative distribution functions of the within-cluster SSE's for different choices of  $C$  (in different colors).

Table S8: Results obtained from the cluster analysis with the Mallows mixture model with Spearman distance, for  $C = 7$ : sushi items arranged according to the MAP estimates of the cluster centers, together with the corresponding MAP estimates for  $\tau$  and  $\alpha$  (with 95% HPD intervals).

Cluster	$c = 1$	$c = 2$	$c = 3$	$c = 4$
$\tau_c$	16.3%(14.3%,17.9%)	12.5%(11.1%,14.7%)	23.1%(17.6%,25.3%)	10.4%(9.24%,12.0%)
$\alpha_c$	0.72(0.67,0.76)	1.47(1.45,1.51)	1.82(1.80,1.86)	2.16(2.14,2.20)
	fatty tuna tuna shrimp tuna roll squid sea eel egg cucumber roll salmon roe sea urchin	sea urchin fatty tuna salmon roe tuna shrimp squid tuna roll sea eel egg cucumber roll	fatty tuna sea eel sea urchin salmon roe tuna shrimp tuna roll squid egg cucumber roll	salmon roe fatty tuna tuna tuna roll shrimp egg squid sea eel cucumber roll sea urchin
Cluster	$c = 5$	$c = 6$	$c = 7$	
$\tau_c$	4.14%(3.48%,4.93%)	4.67%(3.91%,5.63%)	28.8%(26.6%,31.8%)	
$\alpha_c$	2.41(2.39,2.45)	2.86(2.84,2.90)	3.49(3.47,3.53)	
	shrimp salmon roe sea eel squid egg sea urchin cucumber roll tuna roll fatty tuna tuna	egg shrimp squid sea eel cucumber roll tuna tuna roll fatty tuna salmon roe sea urchin	fatty tuna tuna shrimp salmon roe sea urchin sea eel squid tuna roll egg cucumber roll	

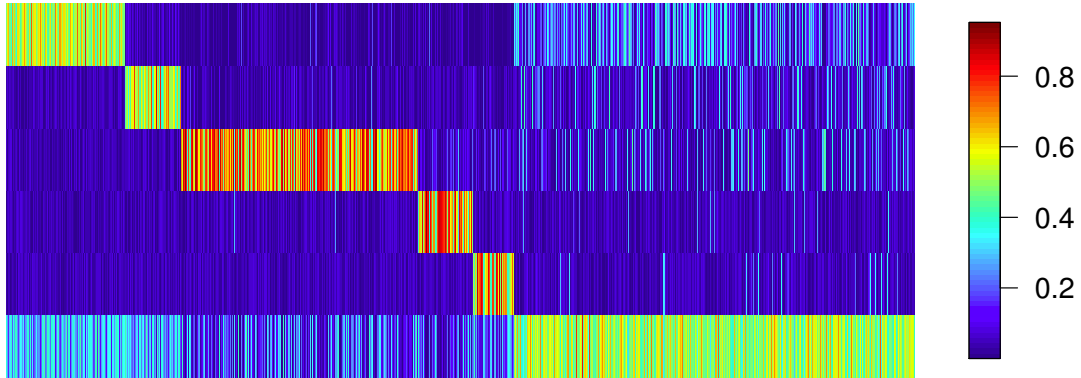


Figure S21: Cluster analysis of the sushi dataset when applying Mallows mixture models with the footrule distance and  $C = 6$ : heatmap of posterior probabilities, for all 5000 assessors, for being assigned to each of the six different clusters identified by the MAP estimate of Table 2.

## D.2 Uncertainty in cluster assignment

We can further inspect the stability of the classification of the individual assessors into different clusters. Considering this question here in the context of models based on footrule distance, we display in Figure S21 the heatmap of posterior probabilities, for all 5000 assessors, for being assigned to each of the  $C = 6$  clusters identified by the MAP estimate of Table 2. As shown by the heatmap, most of these individual level probabilities are concentrated on some particular preferred value of  $c$  among the six possibilities, indicating a reasonably stable behavior in the cluster assignments. The two clusters which show the highest a posteriori uncertainty in the assignment of assessors are the first and the sixth. This is consistent with Figure S22, describing pairwise footrule distances between the MAP estimates of the cluster centers. Here the first and sixth are the clusters whose centers are closest to each other.

## D.3 Convergence checks

Some convergence plots are shown in Figures S24 and S25. In Figure S24 the trace plots of  $\rho_c$  for the first 4500 iterations of the MCMC algorithm are shown for all clusters and for three sushi items: fatty tuna, which is always ranked high, cucumber roll, which is generally disliked, and shrimp, which is somehow in the middle. The trace plots corresponding to three random starting points are shown for each item. Different colors refer to different clusters. A similar plot is shown in Figure S25 for  $\alpha_c$  and  $\tau_c$ .

## E School data

The school data were collected by Prof. Roberta Micheli in the school years from 2002/2003 to 2005/2006, from her class in mathematics at the technical high school "ITIS A. Volta" in Lodi, Italy. Table S9 shows the original data used in the analysis of time-dependent ranks in Section 8 of the main paper. Cells marked NA indicate missing values.

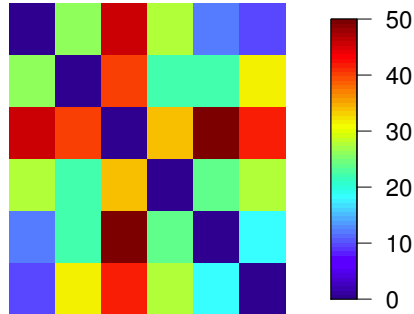


Figure S22: Cluster analysis of the sushi dataset when applying Mallows mixture models with the footrule distance and  $C = 6$ : pairwise footrule distances between the MAP estimates of the cluster centers.

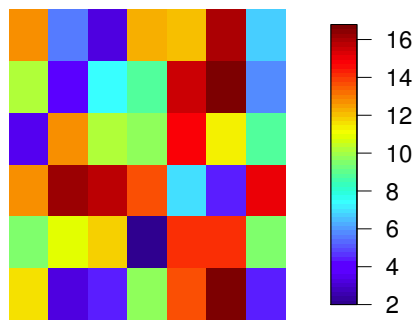


Figure S23: A comparison of results of cluster analysis of the sushi dataset: pairwise Spearman distances between the MAP estimates of the cluster centers when applying the Mallows mixture model with the footrule distance and  $C = 6$  (along rows), and the Mallows mixture model with the Spearman distance and  $C = 7$  (along columns).

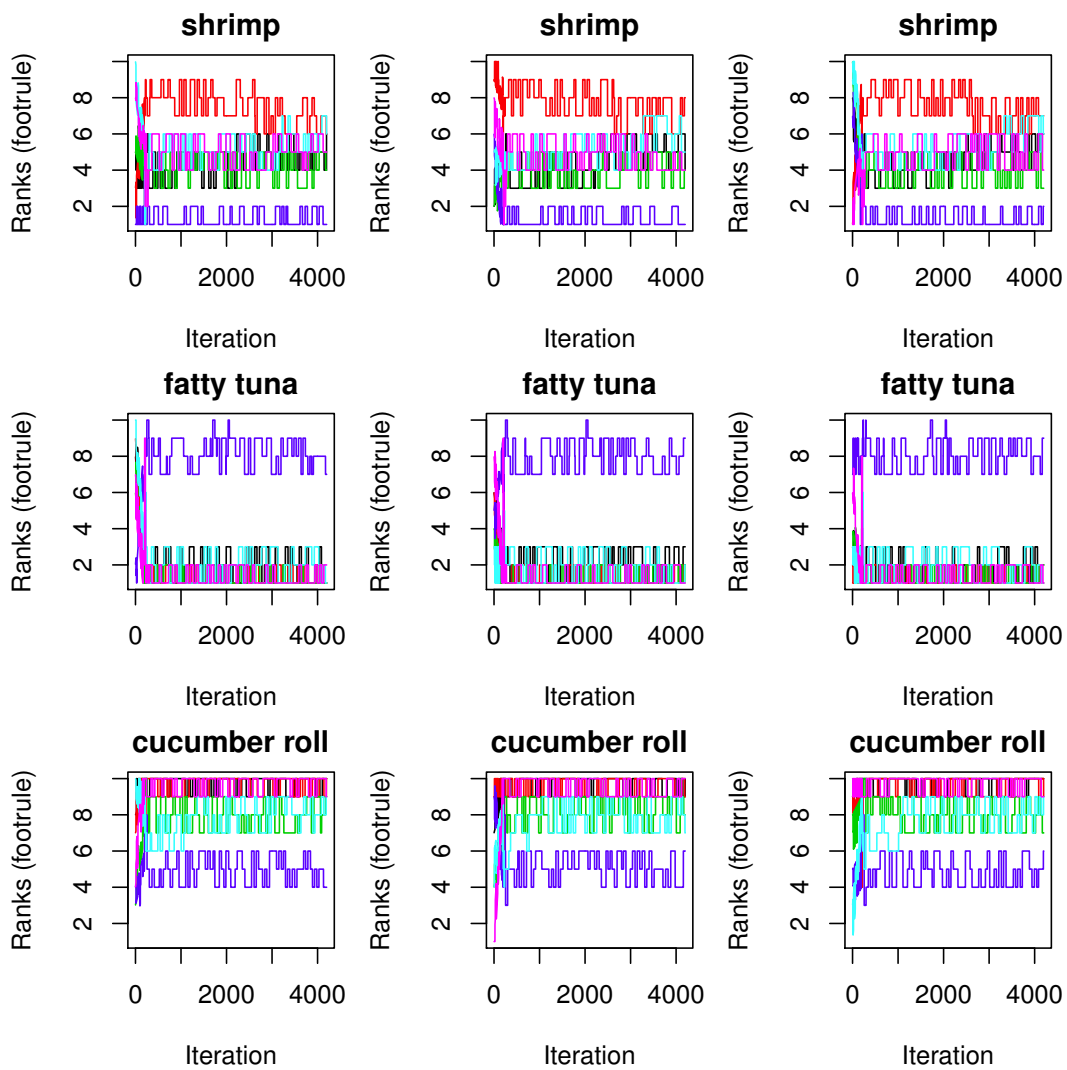


Figure S24: . Cluster analysis of the sushi dataset when applying Mallows mixture models with the footrule distance and  $C = 6$ : trace plots of  $\rho_c$  for the first 4500 iterations of the MCMC algorithm for three sushi items (shrimp, fatty tuna, cucumber roll), and using three random starting points. Different colors refer to different clusters.

Table S9: Test results for each of the 15 students over the 4 years. The individual tests are denoted T1, T2, up to T25.

	Year 1					Year 2					Year 3					Year 4									
	T1	T2	T3	T4	T5	T6	T7	T8	T9	T10	T11	T12	T13	T14	T15	T16	T17	T18	T19	T20	T21	T22	T23	T24	T25
1	5.5	5.3	5.3	9.5	9.0	9.0	8.0	6.3	NA	6.3	6.0	7.8	NA	5.5	7.3	7.3	6.3	NA	6.5	8.5	8.5	8.5	8.5	NA	7.75
2	6.5	6.5	6.8	NA	8.0	6.5	8.0	6.0	7	5.8	5.3	6.5	6.5	NA	6.3	6.3	6	4.5	4.5	6.25	5.75	7	7.0	4	5.75
3	7.5	5.5	8.0	6.8	8.0	7.25	6.0	6.3	8	7	7.5	6.0	NA	5.3	8.5	8.5	7.3	8	6.75	6.75	6	5.75	6	5.75	6
4	5.5	NA	6.8	5.5	4.5	5.0	6.8	5.8	6.5	6	4.8	6.0	NA	4.3	4.0	4.0	5	7.25	NA	7.25	6	5.75	5.5	6.5	6.5
5	4.5	6.8	6.0	7.3	7.5	6.5	7.5	4.3	7	5.8	6.0	7.3	5.5	4.5	7.5	7.5	6.5	5.5	6.5	7.5	8.25	7.5	7.5	5	7.75
6	7.0	8.5	8.0	10	10.0	10.0	10.0	9.0	9.3	8.3	7.0	9.5	9	8.3	9.0	9.0	10	10	9	9.5	8.75	9.5	9.5	8.5	8.5
7	7.0	7.3	8.5	10	8.8	8.5	10.0	6.0	8.3	9.5	8.0	8.0	9.5	8.3	9.5	9.5	9.5	9.25	9.5	9.5	9	9.5	9.5	8.5	9
8	5.5	7	8.0	8.5	7.0	3.75	9.0	7.0	6.3	5.5	6.5	7.3	6	6	8.0	8.0	8.3	5.25	5.25	5.5	8	7.5	6.0	5.75	5.25
9	7.8	6.8	8.0	9.5	9.5	9.0	10.0	8.3	7.8	7.3	9.0	8.5	7.8	8.3	9.3	9.3	8.5	9.5	9.25	NA	7	8.75	8.25	8	7.75
10	4.0	6.5	7.8	7.3	8.0	6.0	7.3	6.0	8.5	5.3	6.0	7.8	7.3	3.5	5.0	5.0	6.5	6.5	5.25	6	NA	6.5	7.5	4	5.75
11	4.0	4.5	4.3	5	5.5	3.5	5.0	3.0	6.5	5	6.0	7.0	5	5.3	4.5	4.5	NA	5.25	NA	6	4.75	6	5.5	3	5
12	5.5	5	9.0	8.3	5.5	4.5	7.0	4.5	9.3	6.8	6.5	6.5	6	4.5	5.5	5.5	6	6	7	4.5	5	4	6.25	3	NA
13	6.8	7	7.3	6.5	9.0	7.5	9.5	8.0	9	NA	7.5	7.5	6.8	7.3	8.5	8.5	8.3	8.5	7	8	8.75	8.75	8.25	6	8.25
14	6.5	8	5.0	6	7.0	6.75	7.0	4.3	7	5.8	5.0	6.5	7.8	5	4.5	4.5	6.5	5	4	5.75	5	6.5	5.0	5.5	4.5
15	7.0	6.5	8.0	4.5	6.8	6.5	7.5	7.0	9	6	6.0	7.5	6	NA	8.0	8.0	NA	7.75	4.5	6	6	NA	5.0	8	6.75

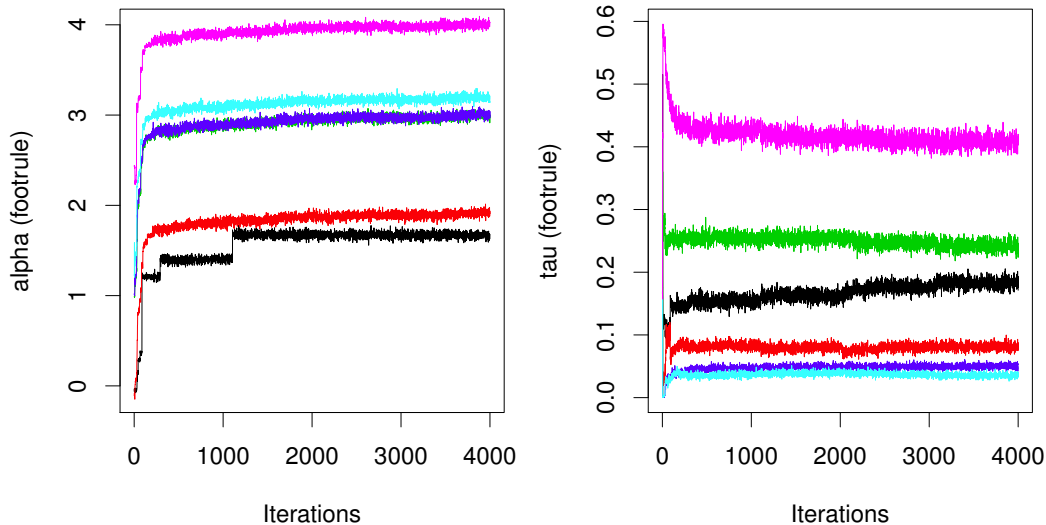


Figure S25: . Cluster analysis of the sushi dataset when applying Mallows mixture models with the footrule distance and  $C = 6$ : trace plots of  $\alpha_c$  (left)  $\tau_c$  (right) and for the first 4000 iterations of the MCMC algorithm using a random starting point. Different colors refer to different clusters.

## F Further simulation experiments

### F.1 Ranks generated from a Mallows model

In addition to the simulations described in Section 9 of the main paper, we conducted further experiments in which the ranks were generated from the three Mallows models with the footrule, Kendall, and Spearman distance. We did this by forward simulation from the generative distribution

$$P(\mathbf{R}|\alpha, \rho) = Z_n(\alpha, \rho)^{-1} \exp \left\{ \frac{-\alpha}{n} d(\mathbf{R}, \rho) \right\}.$$

We set the number of assessors to  $N = 10$ , and the number of items to  $n = 20$ . For each value of  $\alpha$  in a discrete range, we used the Metropolis-Hastings algorithm with fixed ranks  $\rho = (1, \dots, n)$  and fixed  $\alpha$  to obtain  $N$  simulated samples. This was done by first running the algorithm until convergence, and then taking  $N$  observed ranks with a large enough interval between each sample to make them nearly independent. This gave a set  $\mathbf{R}_1, \dots, \mathbf{R}_N$  of observed ranks. This set of ranks was then analyzed by the Mallows models with the three distance measures, using the prior distributions described in Section 2.2 of the main paper. This gave three posterior distributions of ranks, one for each distance measure. We finally found the mean distance from the ranks for each of these three sets of ranks. We thus had a  $3 \times 3$  design, with three Mallows models for generating samples and three Mallows models for analyzing the observed ranks. The procedure was repeated 100 times for each value of  $\alpha$  and each of the 9 settings. The values of  $\alpha$  used for generating the observed ranks were 1, 2, 3, 4, 5, 6, 8, 10, 12, 14 for the Mallows model with footrule and Kendall distance, and the equivalent  $1/n, 2/n, 3/n, 4/n, 5/n, 6/n, 8/n, 10/n, 12/n, 14/n$  for the Mallows model with Spearman distance.

Figure S26 shows the mean footrule distance from the posterior means to the true ranks over the 100 simulations. The error bars were very narrow, and hence omitted. Similar plots using

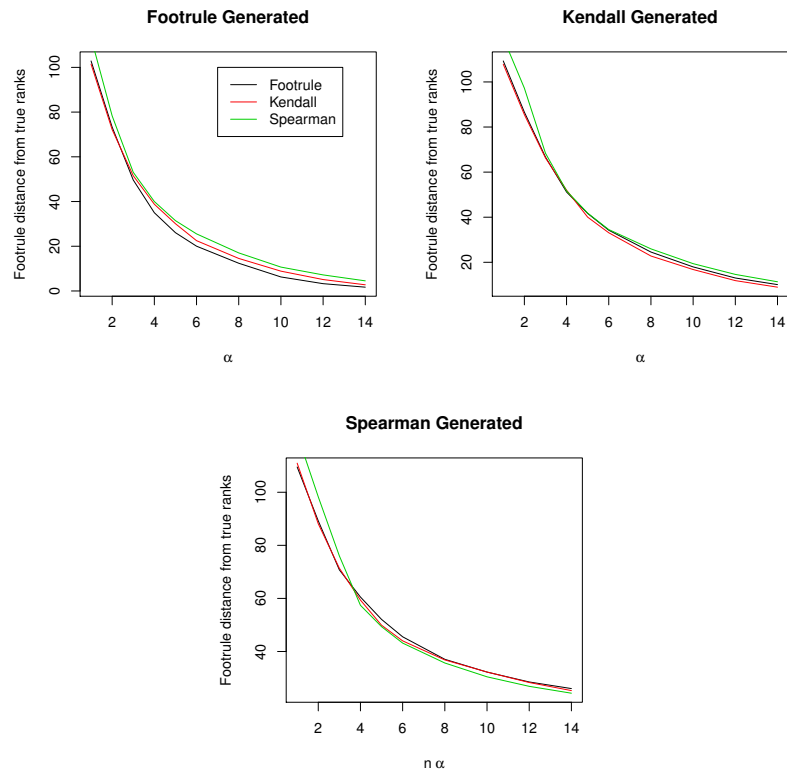


Figure S26: The plots from left to right show the mean distance between the posterior ranks and the true ranks in our simulation experiment, when the observed ranks were *generated* from the Mallows model with the footrule, Kendall, and Spearman distance, respectively. The black curves represent the ranks *estimated* with a Mallows model with the footrule distance, the red curves with the Kendall distance, and the green curves with the Spearman distance.

the Kendall or Spearman distance on the vertical axis gave practically identical results, and are not shown.

The left plot in Figure S26 shows the case in which the Mallows model with the footrule distance was used to generate the samples. In this case, it is clear that inference with the same Mallows footrule model that was used to generate the samples, gave the best results over the whole range of  $\alpha$  values considered, although the difference between the models was rather modest. The center plot shows the case in which the Mallows model with the Kendall distance was used to generate the samples. Here, it is harder to see any difference between the results obtained from the inference with the different Mallows models. For small values of  $\alpha$ , the Mallows model with Spearman distance gave poorer results, while the models with footrule and Kendall distance gave very similar results. For large values of  $\alpha$ , on the other hand, the Mallows model with Kendall distance produced slightly better results than the other two. Finally, the right plot shows the results obtained for the samples generated with the Mallows model with the Spearman distance. Here, it is interesting to see that inference with the footrule and Kendall models was better than with the Spearman model for small values of  $\alpha$ , despite the fact that the samples were generated with the latter model. For  $\alpha$  in the middle and upper range, on the other hand, inference with the Mallows model with the Spearman distance gave slightly better results than the two other models.

These experiments suggest that the Mallows model with the Spearman distance is at a disadvantage when  $\alpha$  is small, i.e., when the ranks are close to being uniformly distributed. For larger values of  $\alpha$ , inference with the same model as was used to generate the data is slightly better than inference with any of the other two models.

## G Convergence of Metropolis-Hastings algorithm

Here we describe how to assess convergence of our Metropolis-Hastings algorithm, using examples from the potato experiment. Similar convergence assessment were performed for all the examples presented in the paper.

### G.1 Potato experiment with full data

Figure S27 shows trace plots of the first 4000 iterations of the MCMC algorithm using the footrule model and the data from the visual inspection experiment. The four plots show the traces for four different starting points. We see that after about 1000 iterations  $\alpha$  has converged to the same distribution in all cases. In each of the four runs, the starting points for the ranks were sampled uniformly from  $\mathcal{P}_n$ . Figure S28 shows the corresponding trace plots for potatoes *A*, *B*, *C*, and *D*. Also here we see that the impact of the initial configuration is negligible after about 1000 iterations. The trace plots of the 16 remaining potatoes gave very similar results (not shown). Keeping in mind that Figures S27 and S28 show traces of different parameters sampled from the same Markov chain, it is interesting to note that only one of the two plots is sufficient to assess convergence. When the algorithm starts,  $\rho$  has little agreement with the data, and therefore  $\alpha$  is drawn towards zero, regardless of the starting point. Eventually, after some hundreds of iterations,  $\rho$  reaches configurations which agree more with the data, and  $\alpha$  therefore increases again. We hence recommend trace plots of  $\alpha$  as a simple tool for assessing convergence. In producing these plots, the proposal distribution for  $\alpha$  was a Gaussian centered at the current value, with standard deviation 0.2. The proposal distribution for  $\rho$  was the leap-and-shift distribution with parameter  $L = 1$ .

Figures S29 and S30 show the same plots for the Mallows model with the Kendall distance and Figures S31 and S32 for the Mallows model with the Spearman distance. These plots also

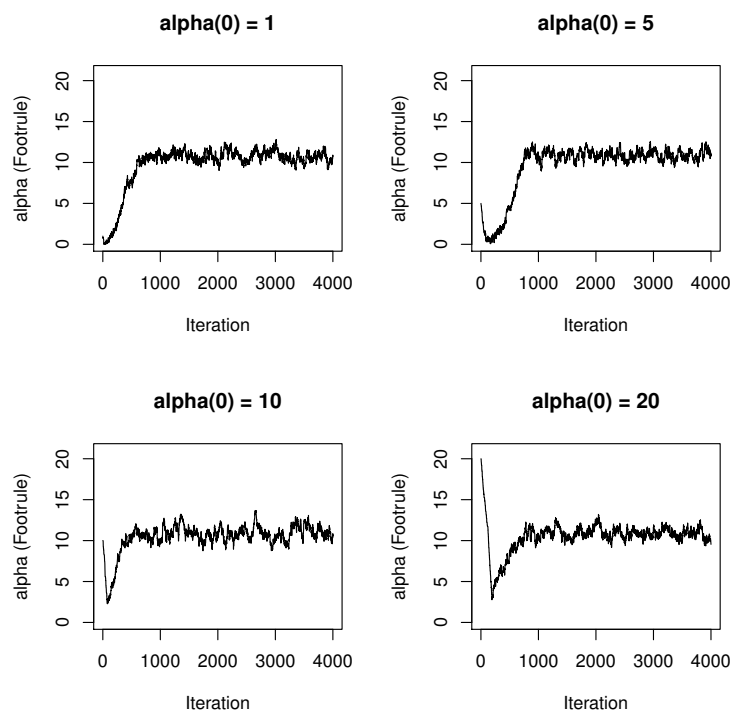


Figure S27: Trace plot of  $\alpha$  for the first 4000 iterations of the MCMC algorithm using four different starting points, 1, 5, 10, and 20, in the Mallows footrule model using data from the visual inspection experiment.

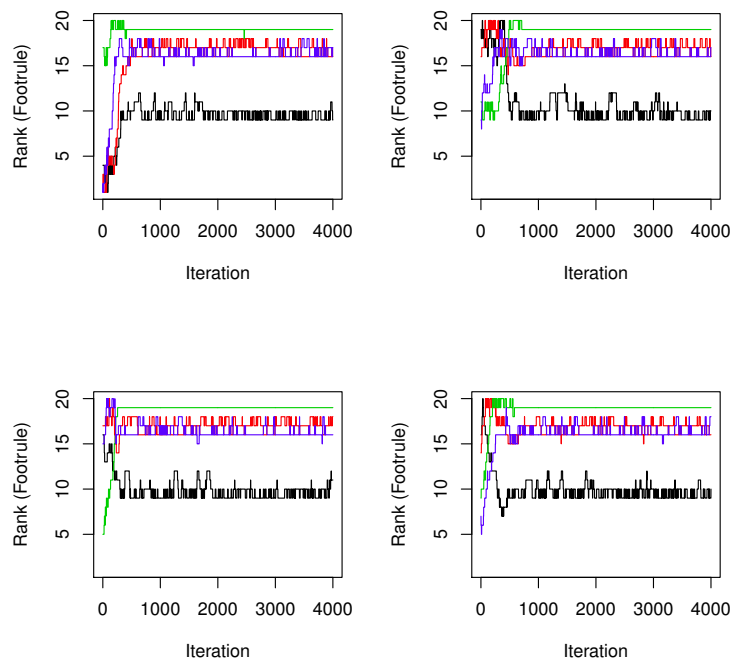


Figure S28: Trace plot of the sampled ranks of potatoes A (black line), B (red line), C (blue line), and D (green line) for the first 4000 iterations of the MCMC algorithm using four different random starting points for the rank vector, in the Mallows footrule model using data from the visual inspection experiment.

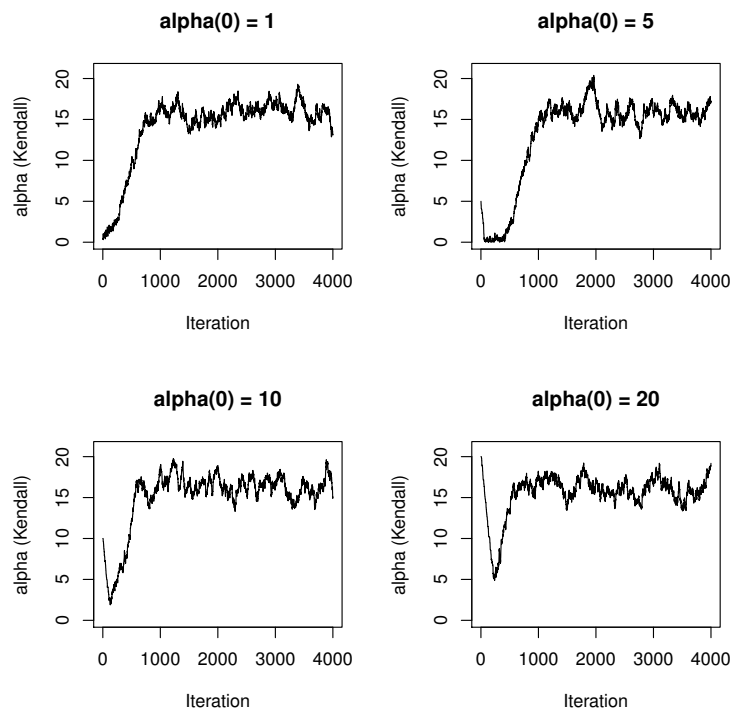


Figure S29: Trace plot of  $\alpha$  for the Mallows Kendall model. See caption to Figure S27.

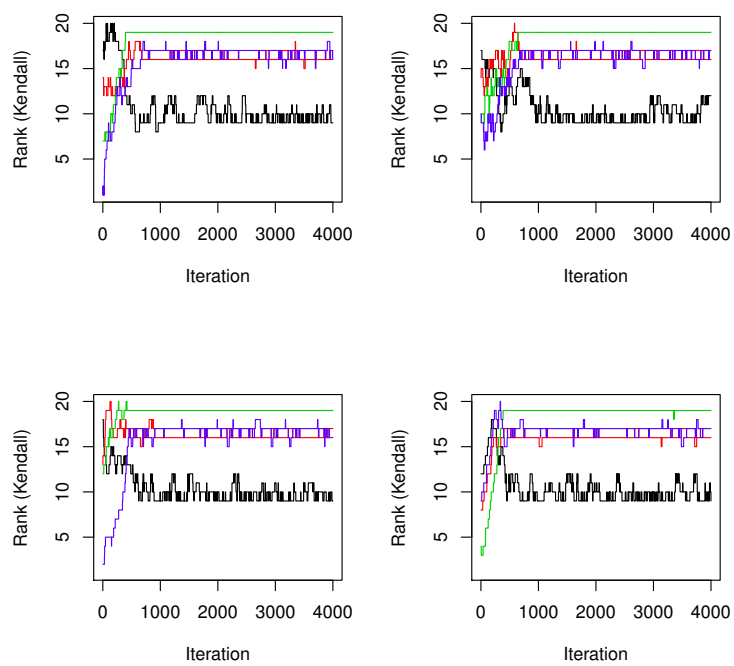


Figure S30: Trace plot of ranks for the Mallows Kendall model. See caption to Figure S28.

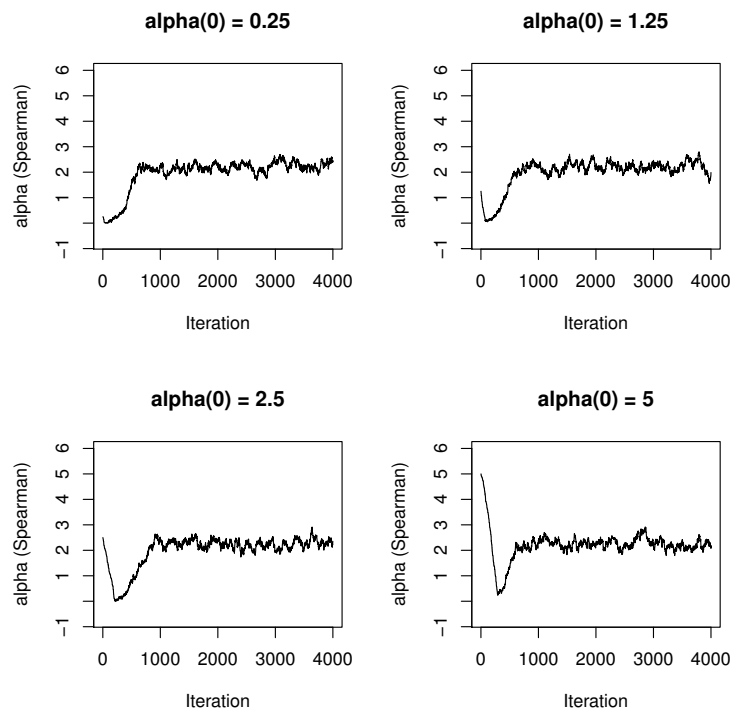


Figure S31: Trace plot of  $\alpha$  for the Mallows Spearman model. See caption to Figure S27.

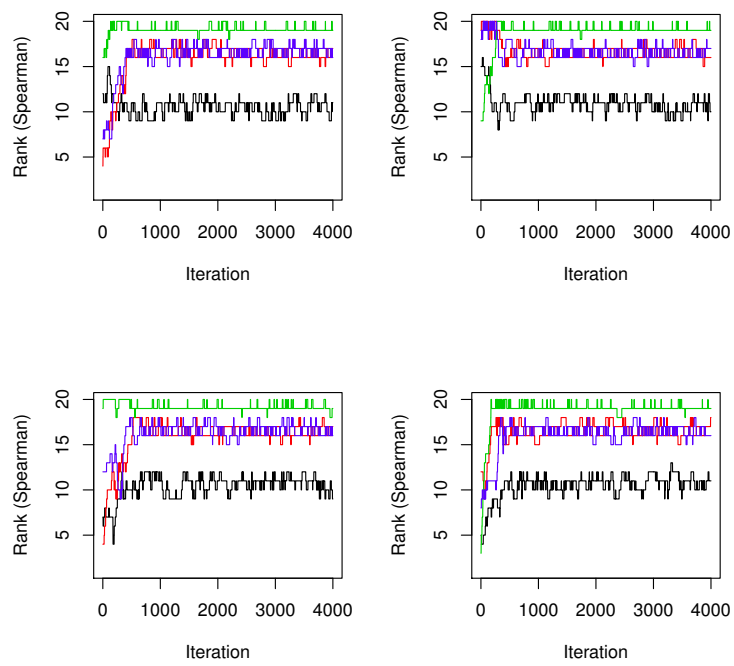


Figure S32: Trace plot of ranks for the Mallows Spearman model. See caption to Figure S28.

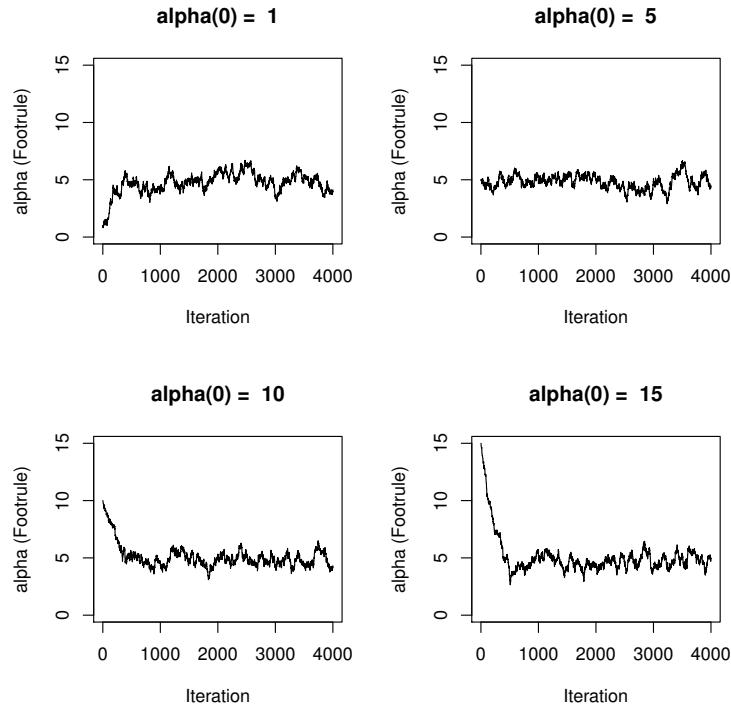


Figure S33: Trace plot of  $\alpha$  for the first 4000 iterations of the MCMC algorithm using four different starting points, 1, 5, 10, and 20, in the Mallows footrule model using top-5 ranks from the visual inspection experiment.

show good convergence after about 1000 iterations. For the Spearman model we used a proposal for  $\alpha$  with standard deviation 0.04, as the value 0.2 used in the two other cases gave a too low acceptance ratio.

Running the 4000 iterations took about 0.01-0.2 seconds on a desktop computer.

## G.2 Potato experiment with top-5 data

Figures S33 and S34 show similar trace plots for the Mallows footrule model when using top-5 ranks in the visual inspection experiment, described in Section 5 of the main paper. We observe that the algorithm seems to converge to its target distribution quickly, and the impact of the initial configuration is negligible after less than 1000 iterations. Running the 4000 iterations on a desktop computer took between 1 and 2 seconds. Although fast, this is slower than for the full data, since a data augmentation is performed in every step of the algorithm.

Similar trace plots were obtained for the Mallows models with Kendall and Spearman distance (not shown).

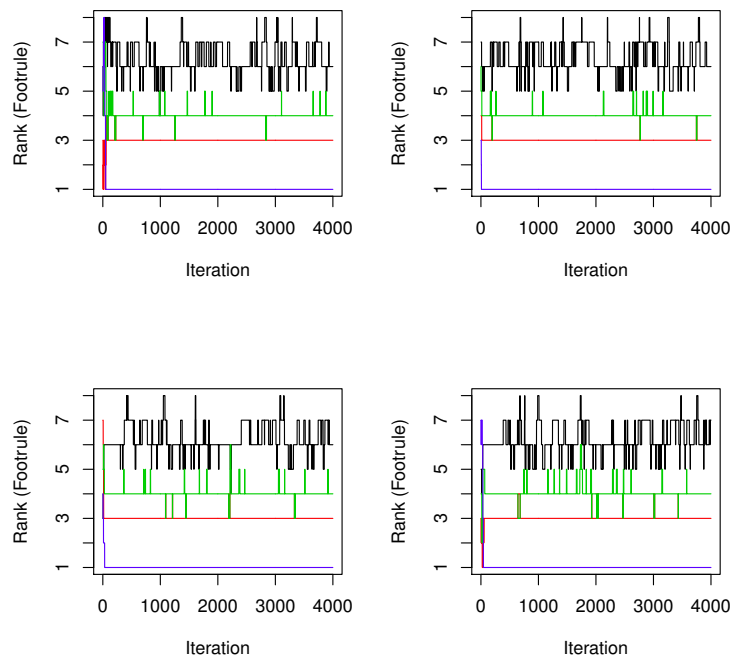


Figure S34: Trace plot of the sampled ranks of potatoes G (black line), I (red line), J (blue line), and L (green line) for the first 4000 iterations of the MCMC algorithm using four different random starting points for the rank vector, in the Mallows footrule model using top-5 ranks from the visual inspection experiment.

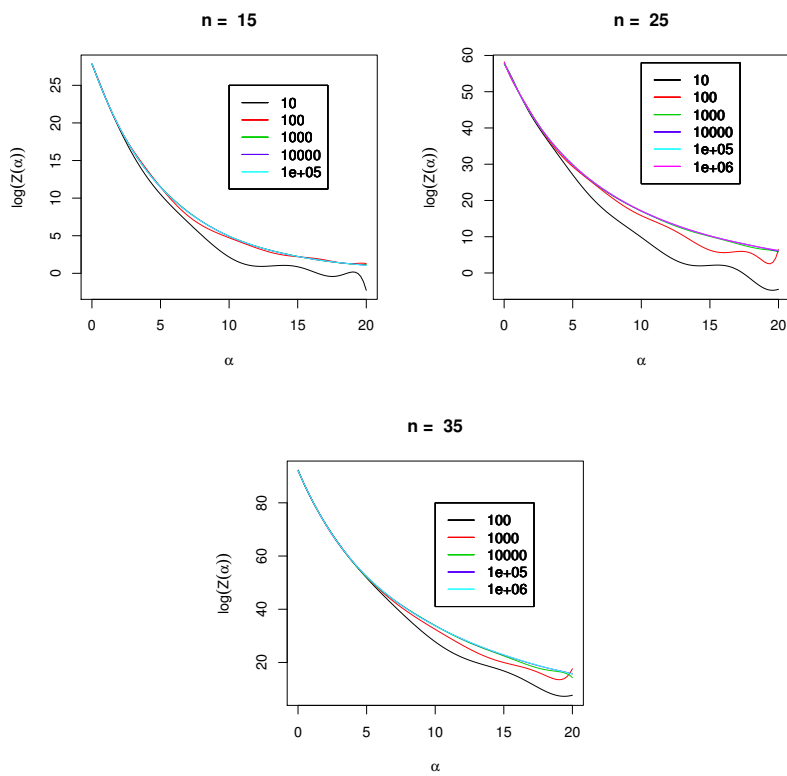


Figure S35: The plots show the estimates of the normalizing constant with the footrule distance using different numbers of Monte Carlo samples, specified by the legend.

## H Convergence of importance sampler

This section illustrates the convergence of the importance sampler, and shows that it produces very good estimates of  $\log(Z_n(\alpha))$  using a number of samples many orders of magnitude smaller than the  $n!$  terms in the exact expression. We present results for the case of the footrule distance, but similar results were obtained for the Spearman distance.

The importance sampler provides an estimate of  $\log(Z_n(\alpha))$ , which we denote  $\log(\hat{Z}_n(\alpha))$ . The accuracy of this estimate increases with the number of Monte Carlo samples. We first confirmed the consistency of the estimator by comparing the estimates to the exact sum for  $n \leq 6$ , seeing that the estimates perfectly overlapped the true function. For larger  $n$ , we determined the number of Monte Carlo samples necessary to obtain a sufficiently accurate estimate, by increasing the number of samples in powers of ten, and computing the difference between consecutive estimates. Between each two estimates, we measured the maximum relative change

$$\epsilon = \max_{\alpha} \left\{ \frac{\left| \log(\hat{Z}_n(\alpha))_{new} - \log(\hat{Z}_n(\alpha))_{old} \right|}{\left| \log(\hat{Z}_n(\alpha))_{old} \right|} \right\} \quad (29)$$

over a discrete grid of 100 equally spaced  $\alpha$  values between 0.01 and 20.0. Finally, we estimated the normalizing constant with a polynomial of degree ten. For some of the examples shown in the paper, the grid of  $\alpha$  values went up to 50.

Table S10 shows the convergence results, and Figure S35 the corresponding estimated curves. In the  $n = 15$  case, the curves based on  $10^3$  and  $10^4$  are indistinguishable, although  $\epsilon$  still is at 0.11 according to the table. Increasing to  $10^5$  Monte Carlo samples,  $\epsilon$  is 0.01. We are thus confident that the final estimate is very good. For comparison, computing the exact value of the normalizing constant would require the summation of  $15! \approx 10^{12}$  terms. For  $n = 25$ ,  $\epsilon$  between  $10^5$  and  $10^4$  samples was 0.03. In order to obtain  $\epsilon$  of at most 0.01, we increased the final number of samples to  $10^6$ , which is much less than  $25! \approx 10^{25}$ .

We conclude from this that the importance sampler yields very good estimates of the normalizing constant using a number of samples which is much smaller than the number of terms in the exact sum. The computations shown here were performed on a desktop computer, and the computation with  $10^6$  samples for  $n = 35$  took about an hour. Generating the Monte Carlo samples used in estimating the sum is perfectly parallelizable, so the computing time has the potential for significant reduction. Alternatively, if the number of samples is in the hundreds, it may be necessary to use parallel computation on a cluster in order to obtain a good estimate in reasonable time.

MC samples	Max. relative change, $\epsilon$		
	$n = 15$	$n = 25$	$n = 35$
10			
$10^2$	277.48	165.24	
$10^3$	0.14	1.48	1.29
$10^4$	0.11	0.07	0.23
$10^5$	0.01	0.03	0.09
$10^6$		0.00	0.00

Table S10: The table shows how the convergence of the importance sampler for the footrule model depends on the number of samples used in the importance sampler. Each row shows the maximum relative incremental error between the current and the previous number of Monte Carlo samples, as specified by (29).